Published in final edited form as:
Nature. 2015 March 12; 519(7542): 187–192. doi:10.1038/nature14259.

Notum deacylates Wnts to suppress signalling activity

Satoshi Kakugawa[#1], **Paul F. Langton**[#1], **Matthias Zebisch**[#2,6,@], **Steve Howell**[1], **Tao-Hsin Chang**[2], **Yan Liu**[5], **Ten Feizi**[5], **Ganka Bineva**[4], **Nicola O'Reilly**[4], **Ambrosius P. Snijders**[3], **E. Yvonne Jones**[2,@], and **Jean-Paul Vincent**[1,@]

[1]MRC's National Institute for Medical Research, The Ridgeway, Mill Hill, London NW7 1AA, UK

[2]Division of Structural Biology, Wellcome Trust Centre for Human Genetics, University of Oxford, Roosevelt Drive, Oxford, OX3 7BN, UK.

[3]Cancer Research UK, Clare Hall Laboratories, Blanche Lane, South Mimms, Potters Bar, Hertfordshire. EN6 3LD, UK

[4]Cancer Research UK, London Research Institute, 44 Lincoln's Inn Fields, London WC2A 3LY, UK

[5]Glycosciences Laboratory, Imperial College London, Department of Medicine Du Cane Road, London, W12 0NN UK

[#] These authors contributed equally to this work.

Abstract

Signalling by Wnts is finely balanced to ensure normal development and tissue homeostasis while avoiding diseases such as cancer. This is achieved in part by Notum, a highly conserved secreted feedback antagonist. Notum has been thought to act as a phospholipase, shedding glypicans and associated Wnts from the cell surface. However, this view fails to explain specificity since glypicans bind many extracellular ligands. Here we provide genetic evidence in Drosophila that Notum requires glypicans to suppress Wnt signalling, but does not cleave their glycophosphatidylinositol anchor. Structural analyses reveal glycosaminoglycan binding sites on Notum, which likely help Notum colocalise with Wnts. They also identify, at the active site of human and Drosophila Notum, a large hydrophobic pocket that accommodates palmitoleate. Kinetic and mass spectrometric analyses of human proteins show that Notum is a carboxylesterase

[@]Authors for correspondence, matthias.zebisch@evotec.com, yvonne@strubi.ox.ac.uk, jvincen@nimr.mrc.ac.uk.
[6]Current address: Evotec (UK) Ltd., 114 Innovation Drive, Milton Park, Abingdon, Oxfordshire OX14 4RZ, UK

Author contributions Experimental contributions were as follows: *Drosophila* developmental genetics (PL, SK); *Drosophila* cell-based assays (SK); Human cell-based assays (MZ, THC); Mass spectrometry (SH, SK, APS); Glycan arrays (YL, SK, TF); Enzymatic assays (MZ); Structural biology (MZ); Peptide synthesis (GB, NO'R). The project was conceived by SK, PL, MZ, EYJ, and JPV. The first draft of the paper was written by MZ, EYJ and JPV with substantial contributions from PL, SK, and APS. All authors contributed to the design and interpretation of experiments.

Supplementary Information is linked to the online version of the paper at www.nature.com/nature.

Methods are linked to the online version of the paper at www.nature.com/nature.

Author information Data deposition statement: The wwPDB accession numbers for the crystal structures reported in this paper are 4wbh, 4uyu, 4uyw, 4uzl, 4uyz, 4uz1, 4uz5, 4uz6, 4uz7, 4uz9, 4uza, 4uzq, 4uzj, and 4uzk.

that removes an essential palmitoleate moiety from Wnts and thus constitutes the first known extracellular protein deacylase.

Keywords

Notum; Wingful; Wnt; palmitoleate; glypicans; feedback inhibition; extracellular deacylase; crystal structure

Negative feedback characterises biological signalling[1] and although often cell-intrinsic, is also mediated by secreted proteins. Cell- and non cell-autonomous feedbacks modulate signal transduction by Wnts, a class of secreted proteins characterised by the presence of palmitoleic acid appended on a conserved serine[2,3]. This palmitoleic acid moiety is essential for signalling[2,4,5], contributing to interaction with Frizzled receptors[3,6,7]. Canonical Wnt signalling triggers expression of intracellular, extracellular and membrane-localised inhibitors of the pathway. Secreted inhibitors include Dkk family members, which bind to the extracellular domain of the Wnt coreceptor LRP5/6, as well as WIF1 and sFRPs, which sequester Wnts[8]. Tiki is a membrane-bound protease that cleaves the N-terminal region of Wnt ligands[9]. Notum is also thought to act enzymatically[10,11] but on glypicans, a class of heparin sulphate proteoglycans (HSPGs) implicated in the extracellular stabilisation, movement, and/or surface retention of Wnts, as well as of other signalling ligands[12-14].

Notum orthologs are found in metazoans from planarians to humans and all bear the hallmark Ser-His-Asp catalytic triad of α/β-hydrolases[10,11]. Notum's sequence similarity to plant pectin acetylesterases prompted the early suggestion that it could hydrolyse glycosaminoglycan (GAG) chains of glypicans[10,11], thus affecting their ability to interact with Wnts and somehow modulating signalling activity. It was subsequently reported that Notum triggers glypican shedding from cultured cells, perhaps by cleaving their GPI anchor[15,16]. Indeed, the currently accepted view is that Notum is a glypican-specific phospholipase[17]. However, glypican-based interactions also modulate Dpp (*Drosophila* TGFβ), Hedgehog, and fibroblast growth factor, as well as Wingless signalling[12-14]. One would expect therefore that these pathways would also be sensitive to Notum-induced glypican release. Yet, existing evidence suggests that Notum is primarily a feedback inhibitor of Wnt signalling. In planarian worms, *Drosophila*, zebrafish and hepatocarcinomas, *notum* expression is activated by Wnt signalling and, conversely, Notum seems to preferentially suppress Wnt signalling[10,11,18-21]. Since more pleiotropic effects would be expected from an enzyme that targets glypicans, we felt compelled to reassess Notum's specificity and mode of action.

Notum specifically inhibits Wnt signalling

To investigate systematically Notum's specificity, we analysed its effects on *Drosophila* wing imaginal discs, which require Wingless (the main *Drosophila* Wnt), Dpp and Hedgehog for patterning and growth[22,23]. As expected, overexpression of Drosophila Notum (dNotum) throughout the dorsal compartment prevented expression of *senseless*, a gene normally activated by high level Wingless signalling. By contrast, *patched (ptc)*, a Hedgehog target gene[24,25], was unaffected (Fig. 1a, b) and phosphoMad (pMad)

Europe PMC Funders Author Manuscripts

immunoreactivity, a marker of Dpp signalling[26], was only mildly reduced (Extended Data Fig. 1a, b). Loss-of-function assays, in homozygous *notum*^{KO} tissue, confirmed dNotum's specificity to Wnt signalling (Fig. 1c, Extended Data Fig. 1c). Although complete loss of *notum* was lethal, strong hypomorphic animals (*notum*^{141} / *notum*^{KO}) survived to adulthood. The wings of such animals had supernumerary margin bristles, consistent with excess Wingless signalling, but had no defects indicative of impaired Hedgehog or Dpp signalling (Extended Data Fig. 1d-g). Nevertheless, extensive evidence suggests that glypicans contribute to these two signalling pathways[27-30]. This is difficult to reconcile with the apparent specificity of Notum if it acts as a glypican-specific phospholipase.

Notum does not cleave the GPI anchor of glypicans

One previously reported observation, namely that dNotum inhibits signalling by membrane-tethered (*i.e.* shedding-resistant) Wingless[11] (Extended data Fig. 2a, b), is incompatible with the view that Notum is a glypican-specific phospholipase. In addition, genetic removal of the two Drosophila glypicans Dally and Dlp did not abrogate high level Wingless signalling (Fig. 1d). These two sets of data strongly suggest that glypican shedding is unlikely to account for the inhibitory effect of dNotum on Wingless signalling. Indeed, we could not confirm the results of an earlier phase partition assay, which suggested that Notum increases the water solubility of glypicans, as expected from GPI cleavage[15]. Extracts from cells expressing tagged Dlp or Dally were treated with either dNotum or bacterial phosphoinositide phospholipase C (PIPLC), an enzyme known to cleave GPI anchors. PIPLC caused both glypicans to partition almost exclusively in the aqueous phase, but dNotum did not (Fig. 1e for Dlp; Extended Data Fig. 2c for Dally) even though, under these conditions, it was effective at inhibiting signalling (Extended Data Fig. 2d). Likewise, in imaginal discs, Notum did not mimic PIPLC: while extracellular Dally and Dlp were noticeably reduced upon addition of exogenous PIPLC, overexpression of dNotum had no such effect (Extended Data Fig. 2e-l). Therefore, experiments with cultured cells and imaginal discs suggest that Notum is not a glypican-specific phospholipase.

Glypicans contribute to the activity of Notum

Even though dNotum does not seem to modulate Wingless signalling by cleaving the GPI anchor of glypicans, genetic interactions between *notum* and *dlp* suggest a functional relationship[31,32]. We therefore investigated the role of Dlp or Dally in dNotum's ability to suppress Wingless signalling. dNotum overexpression, along the anterior-posterior (A-P) boundary, led to complete and long range suppression of Senseless expression (Fig. 2a). In the absence of either Dally or Dlp, this activity was very much reduced, as indicated by the recovery of endogenous Senseless expression (Fig. 2b, c). Notably, Dally was also required for Notum to suppress signalling by membrane-tethered Wingless (Extended Data Fig. 3a). Since Dally is not essential for survival, this requirement could be confirmed in adult wings (Extended Data Fig. 3b-d). To address the relevance of glypican GPI anchorage, we created a transgene expressing Dlp-CD8 (34 C-terminal amino acids of Dlp replaced by the CD8 transmembrane domain) under control of the *tubulin* promoter. This transgene restored the ability of overexpressed dNotum to repress Wingless signalling in *dlp* mutant homozygotes

(Fig. 2d; compare to Fig 2b), confirming the importance of glypicans but not their GPI anchor.

Glypicans bear sulfated glycans. In *Drosophila*, sulfation of the sugar chains requires Sulfateless, a GlcNAc N-Deacetylase/N-Sulfotransferase (NDST)[33], which can be knocked down *in vivo* with an RNAi transgene. Gal4 was used to express this transgene specifically in the posterior compartment, leaving the anterior compartment as a control. At the same time, a *dpp-LexA* driver was used to overexpress dNotum along the A-P boundary. Overexpressed dNotum inhibited Senseless expression in the control compartment but not in the territory deficient in *sulfateless* activity (Fig. 2e). Therefore sulfation of HSPGs is needed for dNotum to act. Notably, overexpressed dNotum did not accumulate in the compartment expressing the *sulfateless* RNAi transgene (compare Fig. 2e' to Fig. 2a'). Likewise, dNotum was depleted from the surface of *dally dlp* double mutant cells generated by mitotic recombination (Fig. 2f). These findings suggest that Dally and Dlp retain dNotum at the cell surface through interaction with their sulfated glycans. Indeed, dNotum bound specifically to sulfated glycans on a glycan array (Extended data Fig. 4). In addition, surface plasmon resonance (SPR) showed that recombinant $hNotum_{core}$ (S81-T451, C330S) bound to heparin and heparan sulfate with micromolar affinities. The dissociation constant of a complex comprising $hNotum_{core}$ and human glypican-3 (GPC3 P31-N538) was 104μM (Fig. 3a). Consistent with the *Drosophila* genetic data, this binding relies largely on the two sulfated GAG chains in GPC3 since their removal led to a more than fivefold reduction in affinity (Fig. 3a). We conclude that sulfated GAG chains on glypicans likely mediate their interaction with Notum.

Structure-guided identification of GAG binding sites

The above results suggest that glypicans contribute to Notum activity by localising it at the cell surface, but are unlikely to be the target of Notum's enzymatic activity. What could the target be? We started to address this question by solving the structures of $hNotum_{core}$ (in nine crystal forms at resolutions between 1.4 and 2.8Å: see Supplementary Information) and of $dNotum_{\Delta loop}$ (in two crystal forms at resolutions of 2.4 and 1.9Å) (Fig. 3b, Extended Data Fig. 5, and Supplementary information). The structures exhibit a canonical α/β hydrolase fold[34], as predicted[10,11]. The conserved 8-stranded central β-sheet is extended on both sides by strands 4 and 14 and is flanked by the canonical six α-helices. This single domain topology is further extended by additional α-helices, two very short β-sheets, several long loops and seven stabilising disulfides. The catalytic triad comprises S232, D340 and H389 (hNotum residue numbering).

Seven sulfate binding sites were identified in $hNotum_{core}$ crystal form III (Fig. 3c; Extended Data Fig. 6). Among them, one (Sulfate 1) was found by SPR to contribute substantially to Heparin-Notum interactions (Fig. 3d). In addition, co-crystals with short heparin oligomers or sucrose-octasulfate (SOS), a heparin mimic, were generated and analysed. These structural studies and additional biophysical analyses (described in Supplementary information and illustrated in Extended Data Fig. 6) delineated an extensive GAG-binding patch centred on a basic groove between the top of the β-sheet and helix αK (Fig. 3c). Importantly, the GAG-binding surface on Notum is distant from the catalytic triad,

consistent with our earlier evidence that Notum binds to glypicans, but does not act on them enzymatically.

Structural and enzymatic evidence for carboxylesterase activity

The α/β hydrolase superfamily includes proteases, lipases, esterases, dehalogenases, peroxidases and epoxide hydrolases[34]. To identify which of these activities relate most closely to Notum's, we compared the structure of hNotum to those of all known α/β hydrolases (PDBe Fold server[35]). The search returned many weak homologs, including human esterase D[36] and acyl-protein thioesterase 1 (APT1)[37] (Extended Data Fig. 7a). A structure-based search for function using the ProFunc Server[38] also suggested that Notum is a carboxylesterase. Furthermore, the closest non-animal homologs of Notum, the pectin acetyl esterases (PAEs) of angiosperms (sequence identity to hNotum 22%, Extended Data Fig. 7b) are carboxylesterases. We assessed the functional significance of these observations by measuring the activity of $hNotum_{core}$ on *p*-nitrophenyl (pNP) acetate (pNP2), a chromogenic carboxylesterase substrate[39]. Significant activity could be detected (Fig. 4a). This activity was strongly inhibited by Triton X-100, and by phenylmethanesulfonyl fluoride (PMSF), a compound known to covalently modify the catalytic serine of serine esterases and proteases (Extended Data Fig. 8a, b). In contrast, there was no measurable hNotum activity on representative sulfatase, phosphatase, phospholipase C or amidase/protease substrates (Fig. 4a). Addition of SOS or heparin resulted in a modest increase in Notum carboxylesterase activity (Extended Data Fig 8a). The possibility that GAGs also contribute to Notum function by allosteric activation requires further investigation.

As a secreted carboxylesterase that inhibits Wnt signalling, Notum is likely to target a carboxy-oxoester or carboxy-thioester bond present on an extracellular component of the Wnt signal transduction machinery. The linkage between Wnt and palmitoleic acid is the only such chemical bond described to date, suggesting that Notum could target Wnt proteins themselves. To evaluate this possibility, we treated mWnt3A with recombinant $hNotum_{core}$ for specific durations, removed the $hNotum_{core}$ and used a cell-based luciferase assay to measure signalling activity of the remaining mWnt3A. This showed that hNotum inactivated mWnt3A directly, irreversibly and in a time-dependent manner (Fig.4b), while no such activity could be detected on Norrin, a non-lipidated ligand that also acts via the Wnt receptors[40] (Extended Data Fig. 8c).

Remarkably, the Notum crystal structures revealed a large (~380$Å^3$), hydrophobic pocket adjacent to the catalytic triad (Fig. 3b, c). Computational docking showed that this pocket could accommodate long chain fatty acids of up to 16 carbon atoms (C16). The size restriction imposed on saturated fatty acids was functionally assessed by measuring hNotum enzymatic activity on commercially available saturated chromogenic pNP ester substrates of varying chain lengths. The activity of human APT1, a cytosolic thio- and oxoesterase was measured in parallel for comparison. hNotum had a pronounced preference for pNP8 (Fig. 4c), with a micromolar Michaelis constant (Extended Data Fig. 8d, e). The activity for pNP-palmitate (pNP16) was less than 0.2% of that for pNP8. To extend our studies of hNotum specificity beyond commercially available substrates, we employed a competitive inhibition assay, using pNP8 as substrate. Saturated 8-12 carbon (C8-C12) long linear carboxylic acids

had significant inhibitory activity (Fig. 4d) while longer saturated fatty acids had no effect. Interestingly however, strong inhibition was observed with the Wnt-associated *cis*-unsaturated lipids myristoleic (C14) and palmitoleic acid (C16) (Fig. 4d; Extended Data Fig. 8f), but not with palmitelaidic acid, the *trans* isomer of the 16:1 fatty acid (Fig. 4 d). These results confirm that Notum can bind to C14 and C16 carboxylic acids if they contain a C9-C10 *cis* double bond and therefore might hydrolyse the oxo-ester bond linking palmitoleate or myristoleate to Wnts.

Notum deacylates Wnts

To test directly Notum-mediated Wnt deacylation we turned to LC-MS analysis. mWnt3A was purified from conditioned medium (CM), treated with recombinant $hNotum_{core}$ or a mock solution, differentially isotope labelled, and trypsinised. No significant identification could be obtained for the predicted palmitoleoylated tryptic peptide, indicating incompatibility with the LC-MS conditions. Importantly however, following treatment with hNotum, this peptide could be identified and quantified in non-acylated form (Fig. 5a, b and Extended data Fig. 9a, b). Replicate LC-MS measurements and label reversal consistently showed an increase in signal intensity for the hNotum-treated de-acylated peptide whereas control peptides showed no significant change (Extended Data Fig. 9c, d). This suggests that treatment of mWnt3A with hNotum removes the palmitoleic acid moiety thus rendering the relevant peptide more hydrophilic and detectable by LC-MS. Encouraged by these results, we proceeded to assess the activity of hNotum on synthetic peptides. The predicted tryptic peptide from hWnt3A was synthesised in a disulphide bonded form with a palmitoleate group on the relevant serine (Methods). These peptides were treated with recombinant $hNotum_{core}$, or with $hNotum_{core}^{S232A}$, which is predicted to be enzymatically inactive, and the reaction products were analysed by MALDI-TOF. No significant deacylation was detected in $hNotum_{core}^{S232A}$-treated samples while hNotum-treated peptides were found to be extensively deacylated (Fig. 5c, Extended Data Fig. 9e). We conclude from these assays that Notum catalyses the removal of palmitoleic acid, which is normally O-linked to S209 of hWnt3A. We also assayed the effect of hNotum on a synthetic peptide from hSonic Hedgehog, which is N-palmitoylated at the amino terminus. No change in the level of acylation could be detected (Fig. 5d, Extended Data Fig. 9f), confirming that Notum's activity on Wnt is specific, in agreement with our genetic evidence.

To gain structural insight into Wnt-Notum recognition, we co-crystallized inactive $hNotum_{core}^{S232A}$ with a palmitoleoylated disulfide bonded peptide corresponding to hWnt7A (C202-C209). The crystal structure revealed the palmitoleoyl group occupying the active site pocket (Fig. 5e, Extended Data Fig. 9g). Electron density was also evident for the ester bond. No interpretable density was found for the peptide, probably due to disorder. This apparent lack of interaction with the peptide concurs with the general observation that esterases/lipases of the α/β hydrolase family bind only to the acid part of the ester substrate. The carboxylic acid carbon is 3.3Å from the Cβ of the mutated Serine nucleophile, a distance consistent with ideal positioning of the hydroxyl for nucleophilic attack. Classically esterasecatalysed hydrolysis proceeds through a tetrahedral transition state characterized by a negatively charged carbonyl oxygen stabilised by two canonical backbone amides, the oxyanion hole[34]. In hNotum the G127-W128 amide participates in formation of the

oxyanion hole in addition to the canonical S232-A233 and G126-G127 amides, thereby providing optimal stabilisation during the transition state (Extended Data Fig. 9g). The kinked *cis* double bond (C9-C10) of the acyl tail is positioned at the base of the pocket between Ile291, Phe319 and Phe320. We found a similar binding mode for a hNotum–myristoleate crystal structure (Extended Data Fig. 9h). Thus, the binding pocket can accommodate extended carbon tails up to C8/C10 but longer fatty acid chains must be kinked at this point in order to fit in. Saturated fatty acids generally adopt an extended conformation, explaining Notum's preference for palmitoleate and myristoleate (both *cis*-unsaturated lipids kinked at C9-C10) over palmitate and myristate. The pocket entrance (lined by Ser232 and His389) is relatively narrow, but comparisons of all hNotum structures suggest substantial flexibility, compatible with palmitoleate entry and release (Extended Data Fig. 5b). Therefore crystallographic evidence strengthens our observation that Notum is a Wnt-specific deacylase with preference for *cis* unsaturated long chain lipids.

Discussion

Only a small number of secreted proteins, Wnts, Hedgehogs, and Ghrelins, are known to be acylated[41]. In all cases, this post-translational modification is essential for activity and is carried out by dedicated membrane bound O-acyl transferases (MBOATs). Porcupine, the Wnt-MBOAT, appends palmitoleate and shorter *cis* unsaturated fatty acids onto Wnt[42]. We have shown here that Notum specifically deacylates Wnts (Fig. 5f) and is thus the first enzyme known to deacylate an extracellular protein. Notum's specificity can be traced to the shape of its hydrophobic pocket, which can accommodate *cis*-unsaturated fatty acids such as myristoleate and palmitoleate, and the nature of its enzymatic activity, a carboxyl oxoesterase. These characteristics ensure that Notum preferentially acts on Wnts, the only secreted proteins known to be O-palmitoleoyleated on a Serine residue. Notum enzymatically inhibits signalling activity by removing the palmitoleate moiety of Wnts, which contributes directly to receptor binding[3]. Notum could also interfere non-catalytically with formation of the Wnt–Frizzled complex by sequestering the palmitoleate moiety since overexpressed dNotum^{S237A} mildly suppressed Wingless signalling *in vivo* (data not shown). We have found that glypicans are required for Notum function and that Notum binds to the sulfated GAGs of HSPGs. Glypicans also bind to Wnts, and can play stimulatory roles in Wnt signalling[43,44]. However, in the presence of Notum, we suggest that glypicans are also inhibitory by acting as a scaffold that co-localises Notum and its substrate (Wnts) at the cell surface (Fig. 5f).

Our results point to Notum's physiological targets being exclusively Wnt family members. Notum is the only secreted Wnt feedback inhibitor found across the metazoan kingdom, from planarians to humans, although seemingly it is seemingly absent from *C. elegans*. Notum's Wnt-deacylation activity, along with other means of feedback inhibition such as ligand sequestration, receptor blocking, receptor downregulation and proteolytic degradation[9,45-47] undoubtedly contributes to the fine balancing of Wnt signalling both during development, for cell fate specification, and in adults, *e.g.* for stem cell maintenance. Indeed, insufficient or excessive Wnt signalling has been associated with diseases such as neurodegeneration and cancer respectively. Our binding data suggest that Notum could possibly be modulated by dietary *cis*-unsaturated fatty acids. Moreover, since Notum is an

extracellular enzyme with a well defined and large active site pocket, it is likely amenable to chemical inhibition to alleviate conditions associated with insufficient Wnt signalling. Conversely, recombinant Notum could be considered as a biologic to prevent excess Wnt signalling such as in Wnt-driven cancers.

METHODS

Immunostaining and microscopy

The following primary antibodies were used: guinea-pig anti-Senseless (1:1000, gift from H. Bellen), mouse anti-Patched (1:50, Hybridoma bank), rabbit anti-V5 (1:500, Abcam), mouse anti-V5 (1:500, Invitrogen), rabbit anti-p-Smad3 (1:500, Epitomics), mouse anti-Dlp (1:50, Hybridoma bank), rabbit anti-GFP (1:500, Abcam), mouse anti-Wingless (1:200, Hybridoma bank). Secondary antibodies used were Alexa 488, Alexa 555 and Alexa647 (1:500, Molecular Probes). Total and extracellular immunostaining of imaginal discs was performed as previously described [48]. Imaginal discs were mounted in Vectashield with DAPI (Vector Laboratories) and imaged using a Leica SP5 confocal microscope. Confocal images were processed with ImageJ (N.I.H) and Photoshop CS5.1 (Adobe). All confocal images show a single confocal section. Adult wings were mounted in Euparal (Fisher Scientific) and imaged with a Zeiss Axiophot2 microscope with an Axiocam HRC camera. Adult wing size and L3-L4 intervein distance was measured with ImageJ.

Drosophila husbandry and clone induction

All crosses were performed at 25°C except those to generate discs shown in Fig. 1a, b, Extended Data Fig. 1a, 1b, Extended Data Fig. 2g, h, k, l and Figure 2f where larvae were reared at 18°C, the Gal80^{ts} permissive temperature, and then shifted to 29°C, the restrictive temperature, 16h prior to dissection to induce *UAS-notum-V5* expression. To generate mutant clones, larvae were heat shocked for 1hr at 37°C at 60hr (±12hr) after egg laying, except for the cross to generate the disc shown in Figure 2f, which was heat shocked for 1 hr at 37°C at 84hr (±12hr) after egg laying. Large mutant clones were generated by including a *Minute* mutation on the homologous chromosome [49]

Drosophila genotypes

Figure 1a) *Cyo / UAS-notum-V5 ; tub::Gal80^{ts} / +*

Figure 1b) *ap-Gal4 / UAS-notum-V5 ; tub::Gal80^{ts} / +*

Figure 1c) *yw hs-FLP ; notum^{KO} FRT2A / Ubi::GFP M FRT2A*

Figure 1d) yw hs-FLP ; dally^{MH32} dlp^{MH20} FRT2A / Ubi::GFP M FRT2A

Figure 2a) *UAS-notum-V5 / + ; dpp-Gal4 / +*

Figure 2b) *UAS-notum-V5 / + ; dpp-Gal4 dlp^{MH20} / dlp^{MH20} FRT2A*

Figure 2c) *UAS-notum-V5 / + ; dpp-Gal4 dally^{MH32} / dally^{MH32} FRT2A*

Figure 2d) *UAS-notum-V5 / tub::dlp-CD8 ; dpp-Gal4 dlp^{MH20} / dlp^{MH20} FRT2A*

Europe PMC Funders Author Manuscripts

Figure 2e) *lex-OP-notumV5 / en-Gal4 UAS::GFP ; dpp-lexA / UAS-sulf-RNAi*

Figure 2f) *yw hs-FLP / + ; UAS-notum-V5 / ptc-Gal4 UAS::GFP ; dally^{MH32} dlp^{MH20} FRT2A / Ubi::GFP FRT2A*

Extended Data Fig. 1a) *Cyo / UAS-notum-V5 ; tub::Gal80^{ts} / +*

Extended Data Fig. 1b) *ap-Gal4 / UAS-notum-V5 ; tub::Gal80^{ts} / +*

Extended Data Fig. 1c) *yw hs-FLP ; notum^{KO} FRT2A / Ubi::GFP M FRT2A*

Extended Data Fig. 1d) *notum^{141} Ubi::GFP FRT2A / Mkrs*

Extended Data Fig. 1e) *notum^{KO} FRT2A / notum^{141} Ubi::GFP FRT2A*

Extended Data Fig. 2a) *UAS-NRT-Wg / + ; dpp-Gal4 / +*

Extended Data Fig. 2b) *UAS-NRT-Wg / + ; dpp-Gal4 / UAS-notum*

Extended Data Fig. 2e, f, i, j) *dally-GFP* (protein-trap, DGRC 115-064)

Extended Data Fig. 2g) *Cyo / UAS-notum-V5 ; tub::Gal80^{ts} / +*

Extended Data Fig. 2h) *ap-Gal4 / UAS-notum-V5 ; tub::Gal80^{ts} / +*

Extended Data Fig. 2k) *Cyo / UAS-notum-V5 ; tub::Gal80^{ts} / dally-GFP*

Extended Data Fig. 2l) *ap-Gal4 / UAS-notum-V5 ; tub::Gal80^{ts} / dally-GFP*

Extended Data Fig. 3a) *UAS-NRT-wg / + ; UAS-notum dally^{MH32} / dpp-Gal4 dally^{MH32}*

Extended Data Fig. 3b) *UAS-notum-V5 / UAS-notum-V5*

Extended Data Fig. 3c) *sal-G4 / UAS-notum-V5*

Extended Data Fig. 3d) *sal-G4 / UAS-notum-V5 ; dally^{MH32} FRT2A / dally^{MH32} FRT2A*

Generation of *notum* knockout by homologous recombination

notum^{KO} was generated by homologous recombination using reagents and crossing schemes described previously [50]. The homology arms were amplified from *w^{1118}* genomic DNA. The primers GATCGCTAGCCGAGAAAGACACAAACGAAGATCAAC and GATCGGTACCCGATTCGATTACACATAGATATAGAATAG were used to amplify the upstream 5kb homology arm, which was cloned into pTV as an Nhe1-Kpn1 fragment. The primers GATCACTAGTGTTATCAAAAGCGAACGCCGCAATAC and GATCAGATCTCTGGAATTGATTTGATTCGATTGCGGTG were used to amplify the downstream 3kb homology arm, which was cloned into pTV as a SpeI-BglII fragment. *notum^{KO}* deletes 82bp sequence of the first exon which encodes the signal sequence. As expected *notum^{KO}* behaved as a null. It was recombined onto *FRT2A* for clonal analysis.

Transgene to express Dlp-CD8

Dlp-CD8 was made by replacing the C-terminus where the GPI anchor is normally added with mouse CD8 transmembrane domain and GFP. The primers GATGAATTCGGCGCGCCATGCTACATCAGCAGCAACAAC and GCATGCGGCCGCCTCGATTGTCATTGGCCCCG were used to amplify 2193bp of the cDNA encoding a polypeptide lacking Asp734, where GPI is normally appended. This fragment was cloned in frame as an EcoR1-Not1 fragment in UASHRP-CD8-GFP (deleting HRP) and the Dlp-CD8-encoding fragment was then transferred to pMTV5 as an EcoR1-Xho1 fragment. From there it was transferred to pTubulin as a Kpn1-Mlu1 fragment. This transgene rescued viability and wing patterning in *dlp* mutant homozygotes, which otherwise do not survive beyond pupal stages, a strong indication that Dlp does not need to be GPI anchored for normal development.

Expression vectors for cultured Drosophila cells

Drosophila S2 or S2R+ (Drosophila Genomics Resource Centre, DGRC), were cultured at 25°C in Schneider's medium + L-glutamine (Sigma) containing 10% (v/v) fetal bovine serum (FBS; Life Technologies) and 0.1 mg/mL Pen/Strep (Life Technologies). To generate plasmids expressing V5-tagged dNotum, the dNotum cDNA (from Stephen Cohen) was amplified, adding a V5 tag (GKPIPNPLLGLDST) at the C-terminus. This fragment was then inserted into pActin, pUAST or pLotattB[51] to generate pAct-Notum-V5, pUAST-Notum-V5 or pLotattB-Notum-V5 respectively. A stable S2 line expressing V5-tagged dNotum (S2 act-Notum-V5) was generated by transfection of S2 cells with pAct-Notum-V5 and pCoHygro (Invitrogen) followed by drug selection. Wingless was expressed from pTub-Wg, which was prepared by inserting the Wg cDNA from pKS-Wg [52] into pTubulin. HA-tagged Dally was expressed from pAct-Dally-HA, prepared by inserting Dally-HA excised from pMTDally-HA (from Stephen Cohen) into pActin. To conveniently manipulate Dlp's coding sequence, three nucleotides (GTC) were inserted at position 2100-2102 (Nucleotide numbering with the A of first codon at position 1) to introduce a Sal I site in KS-Dlp. This was used to insert DNA encoding an HA tag flanked by Glycine (GYPYDVPDYAG) and thus generate pKS-Dlp-HA. The Dlp-HA was then inserted into pTubulin to make pTub-Dlp-HA.

PIPLC treatment of imaginal discs and cultured cells

Wing imaginal discs were treated with PIPLC as previously described in [53] with some modifications. Briefly discs were dissected from 3rd instar larvae and incubated in Schneider's medium with 10% FBS containing 10 U/ml of PIPLC (Molecular Probes) at room temperature for 30 min. After treatment, the discs were washed three times with Schneider's medium before extracellular staining (no detergent). S2 cells transfected with pTub-Dlp-HA and pActin (mock), or pTub-Dlp-HA and pAct-Notum-V5 as well as the corresponding CM were collected (total vol. 300μl) and treated with PIPLC (final concentration 1 U/ml) for 1.5 hours at 25°C before phase separation.

Phase separation assay

The phase separation assay was performed as previously described with some modifications [54]. After PIPLC treatment, 200 μl of pre-condensed Triton X-114 (Sigma) was added to the reaction mixtures (Triton X-114 final concentration ~2%). The extracts were incubated for 15 min on ice and then centrifuged 10,000g for 10 min at 4°C. The supernatant were transferred to new tubes and warmed at 37°C in a water bath for 10 min. After a second centrifugation (10,000g for 10 min at room temperature), the upper phases (aqueous) and lower phases (detergent) were collected separately and mixed with 4x sample buffer (Life Technologies) for analysis by immunoblotting.

Immunoblotting

Samples were run on 4-12% Bis-Tris NuPAGE gels (Invitrogen) with MOPS buffer. Proteins on gel were transferred onto nitrocellulose membrane using iBlot gel transfer System (Invitrogen). The membranes were washed with dH_2O and blocked with 5% skimmed milk in 0.1% tween-20 PBS (PBS-T) for 30 min at room temperature. Membranes were incubated with primary antibodies (mouse monoclonal anti-V5; Life Technologies, 1:5000 and rat anti-HA; Roche, 1:2500) diluted in 5% milk PBS-T overnight at 4°C and washed with PBS-T 3 times before incubation with HRP conjugated secondary antibodies (anti-mouse or anti-rat; Biorad, 1:5000). Membranes were washed again in PBS-T, developed using ECL prime western blotting detection system (GE Healthcare) and exposed to film.

Glycan array

CM obtained from S2 cells expressing V5-tagged dNotum was overlaid on a focused neoglycolipid-based glycan array containing lipid-linked GAG oligosaccharide probes (see http://www1.imperial.ac.uk/glycosciences/ and references [55,56]) and allowed to bind for 90 min. The array was then washed and stained with V5 tag mouse monoclonal antibody (Invitrogen) followed by biotinylated anti-mouse IgG (Sigma). Binding was detected with Alexa Fluor 647-labeled streptavidin. Fluorescence intensity was quantified and data analysis was performed with dedicated microarray software. No binding was observed using the control medium instead of the conditioned medium or when the anti-V5 was used in the absence of the dNotum medium (data not shown).

Large scale expression of Notum constructs

The cDNA coding for mature hNotum (residues R38-S496) was cloned into the pHLsec vector [57] that adds a C-terminal His6- or His10 tag. After the crystal structure was solved in crystal forms I and II (see below) and the folded region identified, a shorter construct $hNotum_{core}$ comprising S81-T451, C330S, was found to provide higher expression levels, thanks in part to the removal of the non-conserved C330 which provides a free, surface-exposed sulfhydryl. Expression of wild type protein resulted in non-quantitative spontaneous crosslinking of the protein, a problem that was not observed with the C330S variant.

For dNotum, we initially attempted to express D83-T617. However, a large unstructured and nonconserved domain of 22kD (R416-K597) was found to interfere with crystallization. This domain, which was not present in hNotum was deleted and replaced by GNNNG to

generate dNotum$_{\Delta loop}$. Note that it could provide an additional glypican-binding surface since it is highly basic (pI=12.4). Proteins were transiently expressed in HEK293T cells and purified as described [47]. Proteins for crystallization were expressed either in GntI-deficient HEK293S cells or in HEK293 cells treated with kifunensine (1mg/l). Prior to crystallization the proteins were treated with endoglycosidase F1 at a ratio of 1:100. Proteins intended for kinetic studies were stored in 10 mM Tris/HCl pH 7.5, 1mM EDTA, 50mM NaCl, 50% (v/v) glycerol at −20°C.

Surface plasmon resonance equilibrium binding studies

Affinity between variants of hNotum and GPC3 or sulfated GAG was measured at 25°C in 10mM HEPES/NaOH pH 7.5, 150mM NaCl, 0.005% Tween20 using a Biacore T200 machine (GE Healthcare). GPC3 constructs (see below) or sulfated GAGs were coupled to a streptavidin-coated sensor chip via a biotin label and purified Notum proteins were used as analyte. Biotinylated GAGs were produced as described [58]. To produce biotinylated GPC3 we proceeded as follows. The cDNA encoding human GPC3 (full length except for the lack of endogenous signal sequence, P31-N538) or GPC3$_{\Delta GAG}$ (lacking C-terminal stretch that normally contains the GAG attachment sites, P31-F493) was cloned into a variant of the pHLsec vector, which introduces a recognition sequence for the *E. coli* BirA enzyme at the C-terminus. Biotinylation at this sequence tag was performed by co-transfection of HEK293T cells with the GPC3 construct and an *E.coli* BirA expression construct. The synthetic BirA gene was codon-optimized and carried a C-terminal KDEL-tag for retention in the endoplasmic reticulum. The BirA plasmid was used at 20% of total DNA. The expression medium was supplemented with 100μM of sterile biotin prepared as a 2mM stock in PBS. After three days, the CM was cleared from cell debris and repeatedly buffer-exchanged to remove free biotin. The chip surface was precoupled with approximately 10000 resonance units (RU) of streptavidin. Approx. 500 RU of GPC3 was immobilized. The amount of immobilized GAGs could not be measured. After each injection of analyte the chip surface was regenerated with 1M NaCl, 10mM HEPES/NaOH pH 7.5 to return to baseline levels. Data were fit to a Langmuir adsorption model ($B = B_{max}C/(K_d + C)$, where B is the amount of bound analyte and C is the concentration of analyte in the sample. Data was then normalized to a maximum analyte binding value of 100. For the design of heparin binding site mutants, the following considerations were taken into account. If, based on the crystal structure, the hydrophobic part of the side chain (*e.g.* Arg, Lys, His) was estimated to be of no structural importance, then the residue was mutated to serine. In all other cases it was mutated to glutamine (Arg, Lys) or asparagine (His) to keep the overall structure as untouched as possible.

Heparin affinity chromatography

We compared the affinity of hNotum variants for Heparin using a 1 ml HiTrap Heparin HP column (GE Healthcare). The column was equilibrated in 10 mM Tris/HCl pH 8.0. 120 μg of sample protein, diluted into binding buffer, was injected onto the column. After washing of the column with 5 column volumes of binding buffer the protein was eluted in a linear gradient to 1.0 M NaCl over 20 CV. The flow rate was 2 ml/min.

Chromogenic Notum activity assays

Steady state carboxylesterase activity measurements of hNotum were performed in 50 mM MES/NaOH, 100 mM NaCl, pH 6.5 using different chromogenic *p*-nitrophenyl (pNP) esters (SIGMA; number indicates carboxylic acid chain length). Substrate stocks in DMSO were adjusted to concentrations between 20 mM (pNP16) and 2 M (pNP2) and diluted into reaction buffer. In tests using the short and soluble substrates pNP2 and pNP4, the final DMSO concentration was only 0.1%. In tests using longer pNP substrates or in comparative studies the final DMSO and Triton concentration was kept constant at 2.5% (v/v) and 0.5% (w/v) respectively. The required amount of a 20mM substrate stock was first mixed 1:1 with a 20% (w/v) solution of Triton X-100 in reaction buffer. The resulting emulsion was then diluted with reaction buffer and vigorously agitated to avoid precipitation. Reactions were started by addition of 5-10µl of protein at concentrations between 0.1 and 4 mg/ml. Substrate was measured using a Varian Cary 50 spectrophotometer by following the absorption change at 405nm. The extinction coefficient of *p*-nitrophenol in reaction buffer was established to be 4070 $M^{-1}cm^{-1}$. Although Triton X-100 was required to maintain the solubility of long ester substrates and fatty acids, it was itself an inhibitor of Notum (Extended Data Fig. 8a and b). We assume that the hydrophobic region of Triton X-100 has a propensity to bind to the active site pocket. This notion is supported by the observation that the much larger sterol-based detergent CHAPS evokes no inhibition. Based on this assumption of competitive inhibition by Triton X-100 we determined its inhibition constant to be 466µM and used it to calculate a corrected Michaelis constant for pNP8 turnover.

Cell-based Notum activity assays

To assay Wingless signalling in Drosophila cells, a modified TOPFlash vector called WISIR, comprising a TCF-responsive promoter driving Firefly luciferase and a ubiquitous promoter driving Renilla luciferase [59] was used. To assess the repressive activity of dNotum, S2 R+ cells were transfected separately in 6 well plates with pTub-Wg (2 µg), pAct-Notum-V5 (2µg) and WISIR (0.3 µg). The transfected cells were then cultured for 2 days at 25°C and then mixed in equal ratio. Firefly and Renilla luciferase levels were measured 24 hrs later with Dual-Glo luciferase reporter assay system. As controls, cells transfected with WISIR alone or with WISIR and pTub-Wg were mixed with mocked treated cells. Firefly luciferase activity was normalized to *Renilla* luciferase activity and the average of triplicate samples was calculated.

hNotum inhibition of Wnt signalling in mammalian cells was assessed in stably transfected SuperTopFlash (STF) HEK293 cells [60]. These were treated with CM from Wnt3A producing L cells [61] with or without recombinant purified hNotum. To reveal the direct action of hNotum on Wnt we proceeded as follows. Wnt3A CM was dialyzed for 24h against ten volumes of tissue culture grade PBS and then sterile filtered with the aim to remove chelators that might interfere with TALON-binding (see below). To 500 µl of such dialyzed Wnt3a, 5µl hNotum protein or an unrelated control protein (mock) at a concentration of 1mg/mL was added and incubated for the indicated time at room temperature (RT, 23°C). To stop the enzymatic reaction we added 50 µl of fresh 50% slurry of cobalt affinity beads (TALON resin) equilibrated against tissue culture grade PBS and 5µl of 500mM imidazole in PBS. After vigorous shaking the solution was incubated for 1h at

RT on a vertical rotator. Beads containing the His_{10}-tagged hNotum protein were removed by centrifugation (3000g, 5min) and discarded. The supernatant was cleared again by centrifugation at maximum speed (16000g, 5min). 100µl of the reaction solution was then added to STF cells seeded the previous day at 50000 cells per 100µl and per well into 96 well plates. The Wnt-induced luciferase activity was measured after 16-20h using the Glo kit (Promega) and an Ascent Luminoskan luminometer (Labsystems) following the instructions of the manufacturer. Data represent average of quadruplicate measurements ± SD. The incubation time with cells was kept constant for all compared samples.

To asses hNotum inhibition of Norrin signalling, STF cells seeded in 96 well plates were transfected after 24h with 200ng DNA: 60 ng each of hFz4 and hLrp6 plasmids, 30 ng of Tspan-12 plasmid, and 50 ng constitutive *Renilla* luciferase plasmid (pRL-TK from Promega). Cells were stimulated 24 h post transfection with 10 µg/ml recombinant Norrin (manuscript in preparation) which had been preincubated for 24 h with 10 ug/ml hNotum variants or as a control, Fetal Calf Serum (FCS). Firefly and *Renilla* luciferase activities were measured 48 hr later with Dual-Glo luciferase reporter assay system (Promega). Firefly luciferase activity was normalized to *Renilla* luciferase activity and the average of triplicate samples was calculated.

Crystallization, data collection, and structure determination

Concentrated proteins were subjected to sitting drop vapour diffusion crystallization trials employing a Cartesian Technologies pipetting robot and typically consisted of 100-300 nl of protein solution and 100 nl of reservoir solution. A detailed discussion of the multiple conditions in which crystal growth occurred is provided in supplementary information. Standard methods were employed for x-ray diffraction data collection and structure determination, destinctive details for the series of crystal structures are discussed in supplementary information.

Mass spectrometric analysis of the effect of Notum on Wnt3A protein

As a general method to quantify the levels of delipidated Wnt3A protein by LC-MSMS, we used an isotope coded alkylation reaction targeting cysteines to multiplex mass spectrometry signal. One sample was reacted with heavy iodoacetamide (IAA, $^{13}C_2D_2HINO$) and the other with the light version (C_2H_3INO) and consequently, peptide signal doublets appeared at Δ4D per cysteine with peak areas used for relative quantification. Wnt3A protein (500ng, purified from L cell CM by Kevin Dingwell (NIMR) according to[4]) was mixed with purified hNotum (1µl of purified $hNotum_{core}$ at 25 ng/µl) in the following buffer: 20mM Tris-HCl buffer (pH 7.5) containing 500mM NaCl, 0.5mM EDTA, 0.5% CHAPS and 5% glycerol and left together for16 hours at 25°C. The reaction was quenched by addition of 4x LDS sample buffer (Life Technologies). Coomassie blue stained bands from SDS-PAGE were excised from the gel and cut in half and destained by incubating for 45mins with 200mM Ammonium bicarbonate (ABC) / 60% acetonitrile (ACN). To reduce cysteines, buffer was refreshed with the inclusion of 10mM DTT for 15 minutes. After washing, half of the gel pieces were incubated in 20 mM heavy or light IAA in 100mM ABC/ 60% ACN buffer in the dark for 30 minutes. Proteins were digested using a 4 hour in-gel trypsin digestion step in 100mM ABC and then quenched with 0.1% TFA. Equal aliquots of heavy and light

reaction were mixed to generate forward and reverse labelled samples. Duplicate LC-MS analysis was performed using an Ultimate3000 RSLC system coupled to a LTQ-Orbitrap Velos-Pro mass spectrometer (Thermo Scientific). The instrument was operated in an alternating targeted MS/MS and data dependent acquisition mode. CHGLSGSCEVK and the control peptide AGIQECQHQFR were targeted for MS/MS. MS/MS spectra were searched using Mascot v2.3 and identifications imported as a spectral library into Skyline software v2.6.0.6709. Skyline was used for peaks extraction and areas determination

Mass spectrometric analysis of Wnt3A and Shh peptides

Delipidation assays were performed by reacting 3 μg of synthetic peptides (synthesis described in supplementary information) with 1μl of enzyme ($hNotum_{core}$ or $hNotum_{core}^{S232A}$; 25 ng/μl) in 20 mM ammonium bicarbonate buffer (Total vol. 5 μl) for 16 hours at 25°C. The reaction was quenched with 0.1% TFA and samples were desalted using c18 zip tips. Samples were prepared in α-cyano-4-hydroxycinnamic acid in 50:50 water/acetonitrile with 0.1% TFA. MALDI-TOF spectra were acquired using an ABSCIEX 5800 TOF/TOF systems and analysed using data explorer v4.11.

Europe PMC Funders Author Manuscripts

Europe PMC Funders Author Manuscripts

Extended Data

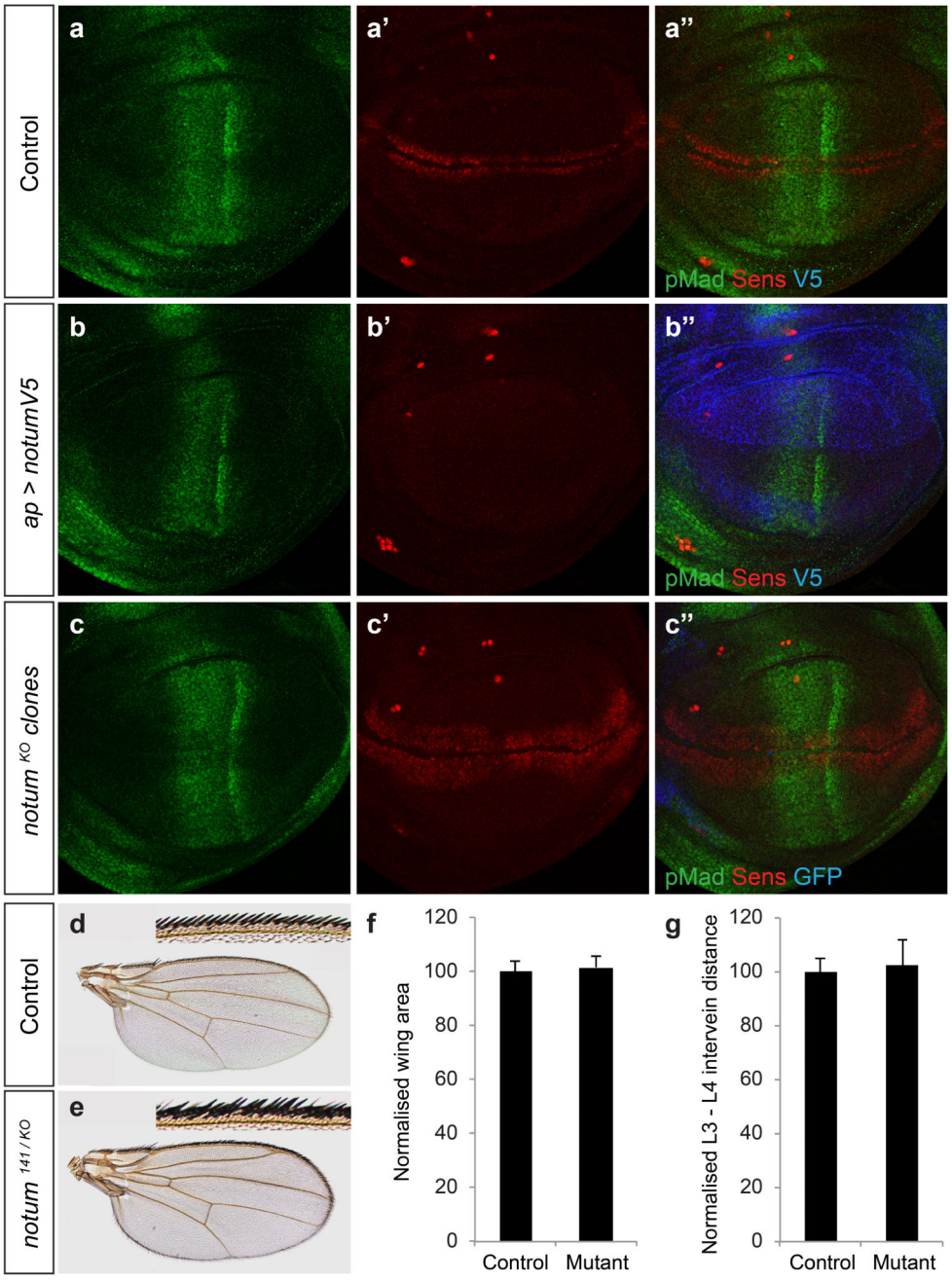

Extended data Figure 1. Notum modulates Wingless, but not Dpp or Hedgehog signalling

a-c, Overexpression of dNotum-V5 with the *apterous-gal4* driver, which is expressed in the dorsal compartment, prevents expression of Senseless (Sens) (b'), a Wingless target gene but has no significant impact on phospho-Mad (pMad) immunoreactivity (b), an indicator of Dpp signalling. Loss of *notum* activity, achieved by generating large patches of *notum*^{KO} tissue (See Methods), marked by the loss of GFP, leads to broadening of Senseless

Europe PMC Funders Author Manuscripts

expression but does not affect pMad immunoreactivity. **d-g,** Strong, but not complete, reduction of *notum* activity led to ectopic wing margin bristles (compare inset in d and e) but had no significant impact on wing area, which is sensitive to Dpp signalling (f) ($p = 0.26$, Student's t-Test), or on the distance between L3 and L4 veins, which is affected by changes in Hedgehog signalling [62] (g) ($p = 0.41$, Student's t-Test). 19 control ($notum^{141/+}$) and 17 mutant ($notum^{141/KO}$) wings were analysed.

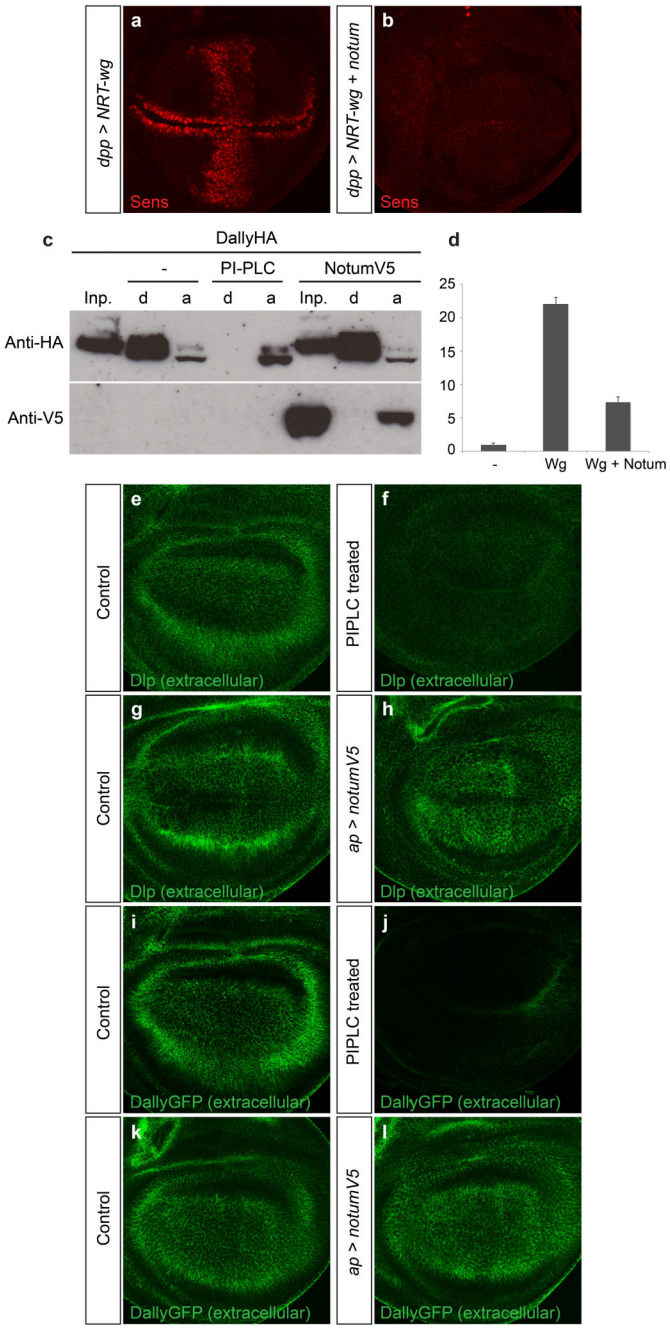

Extended data Figure 2. dNotum does not cleave the GPI anchor of glypicans

a, **b** Ectopic expression of Senseless caused by NRT-Wingless, as well as endogenous Senseless, is suppressed by co-expression of dNotum. NRT-Wingless and dNotum are expressed in a vertical band under the control of *dpp-gal4*. **c**, Western blot analysis of phase-separated extracts of S2 cells transfected with a plasmid expressing HA-tagged Dally. In control extracts, Dally is found largely in the detergent (d) phase. Coexpression of dNotum-V5 from a plasmid had no impact, while treatment with PIPLC shifted all detectable Dally to the aqueous (a) phase. **d**, dNotum-V5 expression as in panel c was sufficient to suppress Wingless-induced TOPFlash activity. Cells were transfected with a dual luciferase TOPFlash reporter [59] along with a mock plasmid (−), *tubulin::wingless* (Wg), or *tubulin::wingless* + *actin::notum-V5* (Wg + Notum). **e**-**h**, Extracellular Dally-like protein (Dlp) in control (e, g) , PIPLC-treated (f) or *apterous-Gal4 UAS-notum-V5* (h) imaginal discs. **i**-**l**, Extracellular anti-GFP staining of imaginal discs from gene trap line expressing Dally-GFP fusion protein. Discs treated with a mock solution (i) or PIPLC (j) (same discs as in e and f respectively but here showing Dally protein). In a separate experiment, dNotum was overexpressed with *apterous-Gal4* in the *Dally-GFP* background (l). No change in the distribution of extracellular GFP could be seen compared to that in control discs (k, no *apterous-Gal4)*

Europe PMC Funders Author Manuscripts

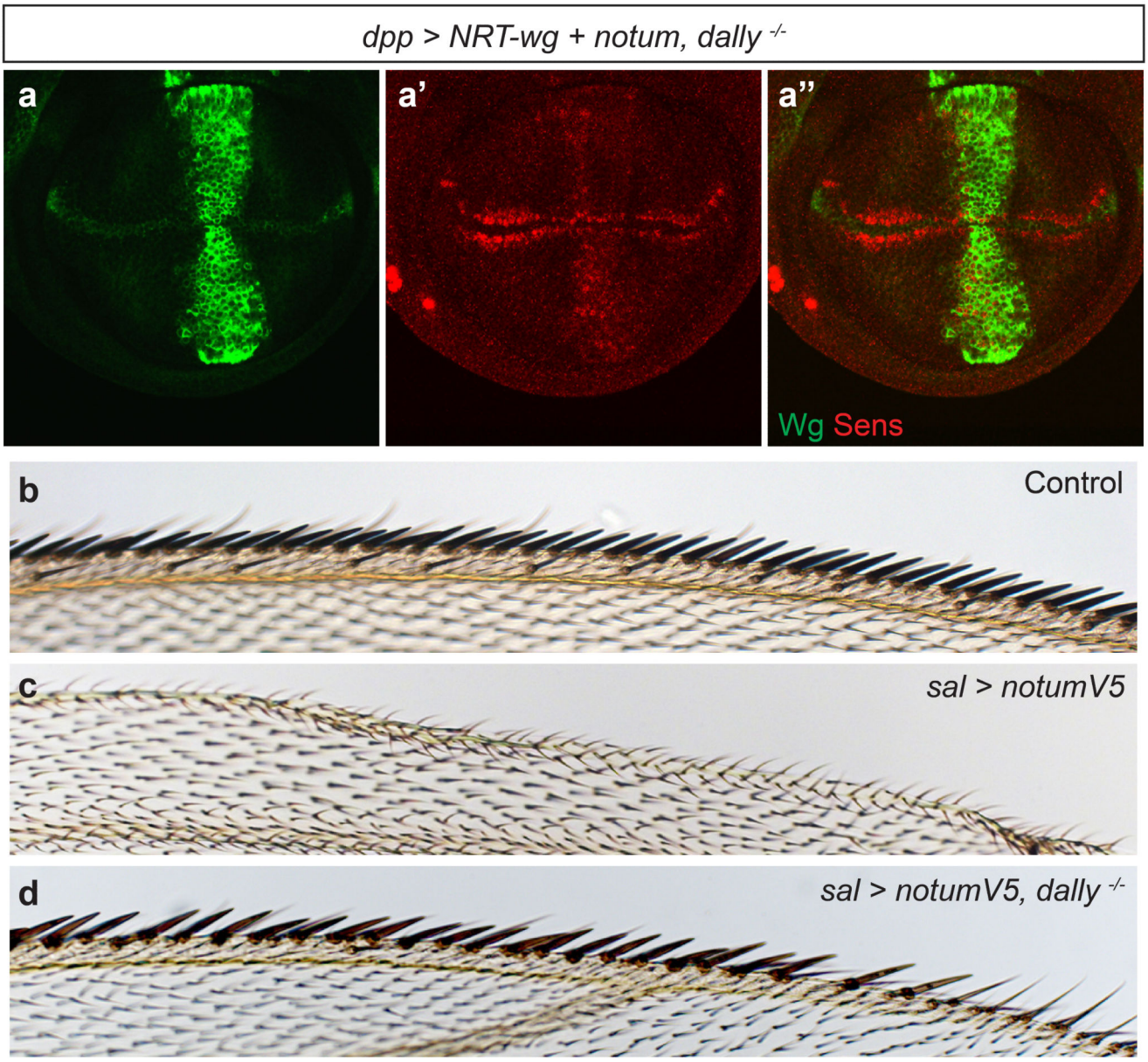

Extended data Figure 3. dNotum requires Dally to inhibit Wingless signaling

a, Wingless and Senseless expression in a *dally*$^{-/-}$ wing imaginal disc expressing *NRT-wingless* and *notum* under the control of *dpp-Gal4.* Some *senseless* expression remains, indicating that, in the absence of Dally, dNotum is a poor inhibitor of NRTWingless-induced (as well as endogenous) signalling. **b-d**, Anterior margin of wings from control, *spalt (sal)-Gal4 UAS-notum-V5*, and *sal-Gal4 UAS-notum-V5 dally*$^{-/-}$ animals. Removal of *dally* rescues the loss of margin bristles caused by dNotum overexpression.

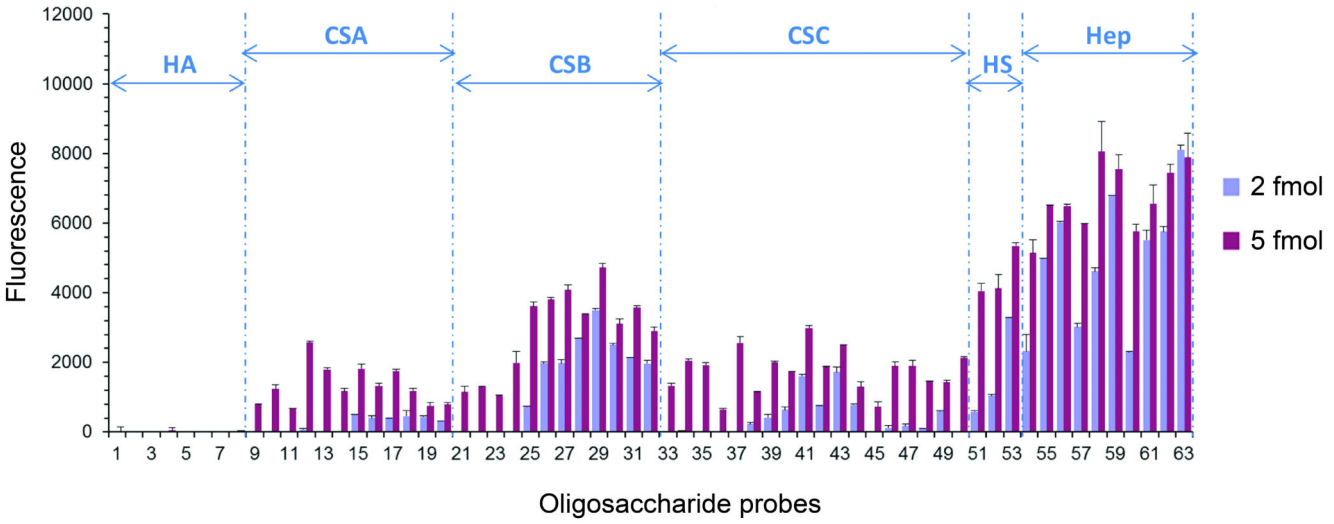

Extended Data Figure 4. dNotum binds to sulfated glycans

Binding of dNotum-V5 to a GAG oligosaccharide array, detected by immunofluorescence. HA = Hyaluronic acid, CSA/B/C = Chondroitin Sulfate A/B/C, HS = Heparan Sulfate, Hep = Heparin. Details on the array are provided in Methods.

Europe PMC Funders Author Manuscripts

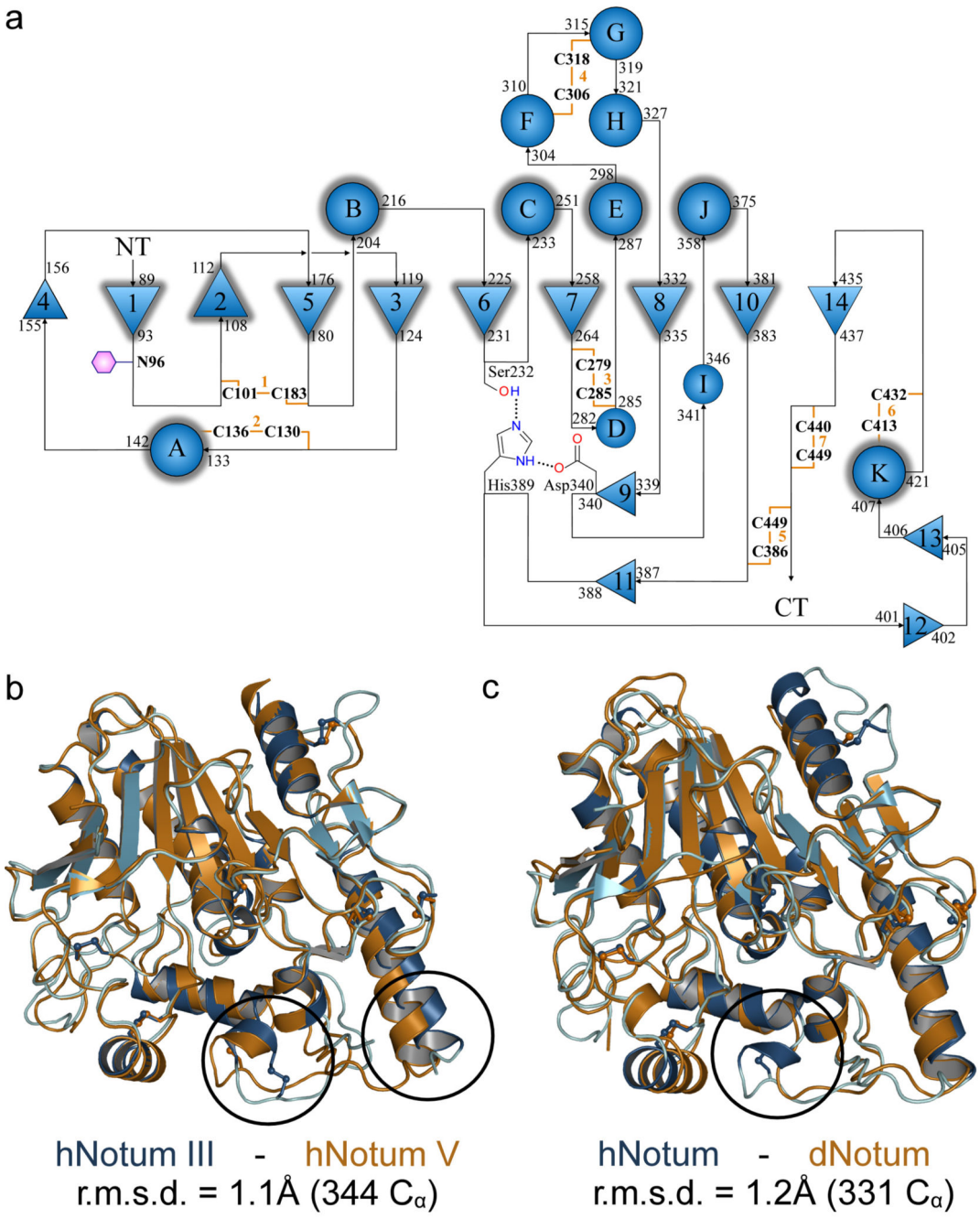

Extended Data Figure 5. Additional structural information on Notum

a, Topology plot of hNotum. β-strands are shown as numbered triangles and α-helices as circles labelled in alphabetical order from the N to C terminus. Structural elements conserved among most α/β-hydrolases are outlined in grey. **b,** Comparison of the two most conformationally distinct hNotum structures (from crystal forms III and V). Crystal form III is the most structurally different. All other structures superimpose with r.m.s.d.s of <0.7Å. The circle highlights the most flexible region. **c,** Comparison between the structures of

Europe PMC Funders Author Manuscripts

hNotum (Form V) and dNotum (Form I). The circle highlights the lack of a cysteine bridge in dNotum.

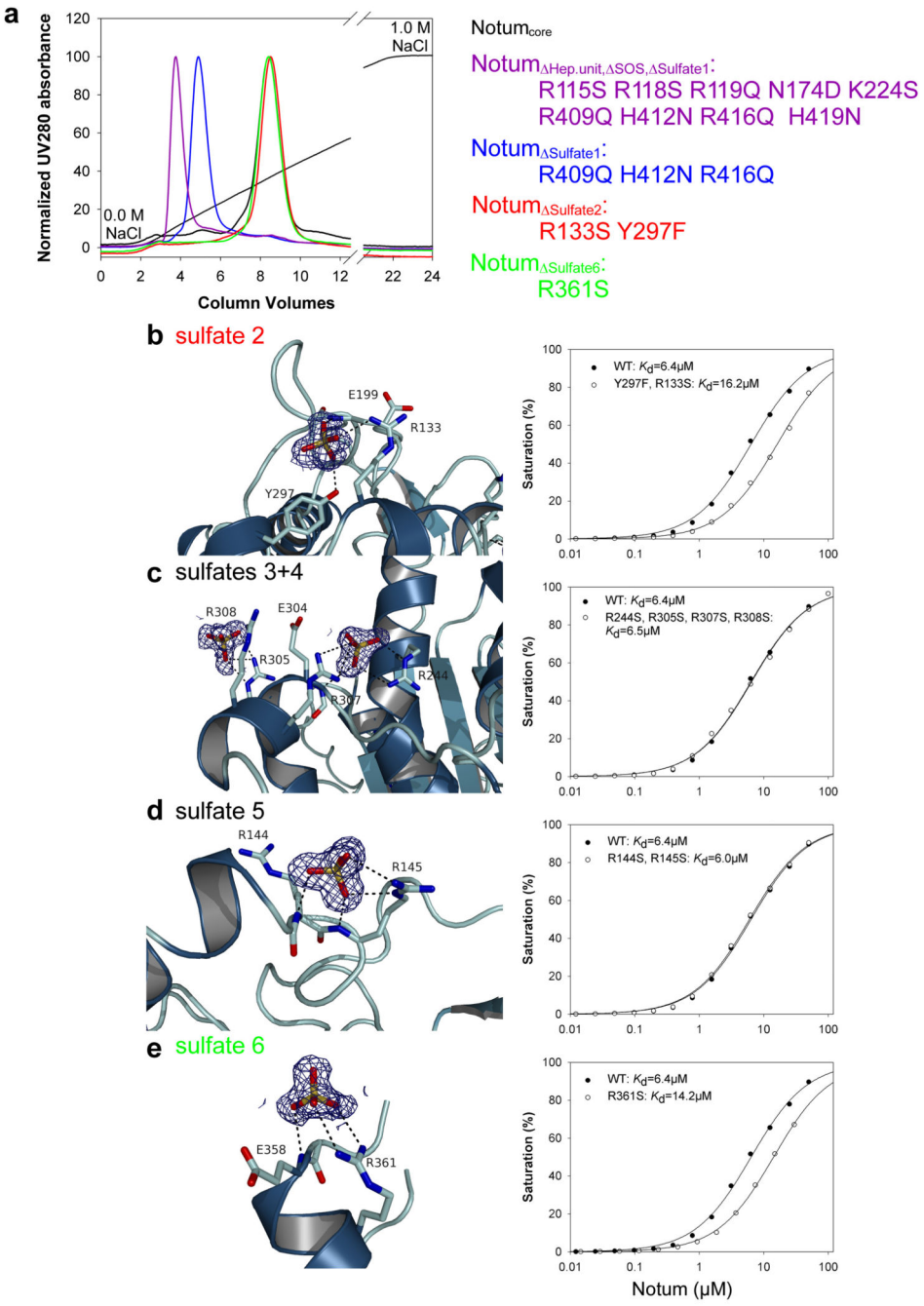

Extended Data Figure 6. Structural and biophysical analysis of heparin binding

a, Heparin affinity chromatography of wild type hNotum and selected surface variants. **b-e,** Close-up views of additional sulfate binding sites on hNotum, crystal form III. Each view is accompanied with SPR heparin affinity data corresponding to each hNotum variant.

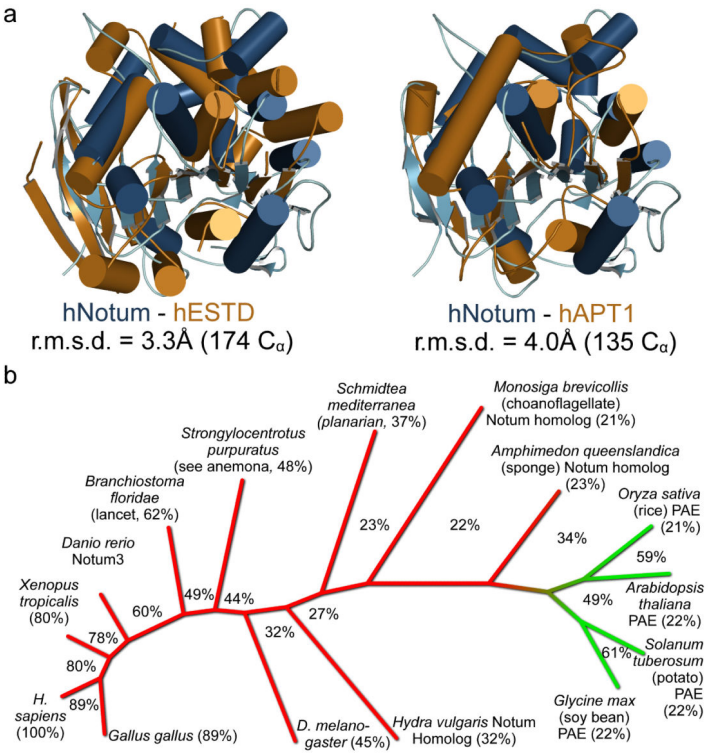

Extended Data Figure 7. Relation of Notum to other Esterases of the α/β hydrolase family

a, Comparison between hNotum and human Esterase D, showing structural relatedness. hNotum is also related to APT1, a cytosolic esterase used in this study as a positive control for fatty acid esterase activity. In the views shown here, the hNotum structure has been rotated by 90° around the x-axis relative to the structure shown in Figure 3b. **b,** Rootless phylogenetic tree of animal Notum proteins (red) and plant pectinacetylesterases (PAE, green). Extent of sequence identity to hNotum is shown next to species name. Percentages between branches indicate sequence identity between neighbours.

Europe PMC Funders Author Manuscripts

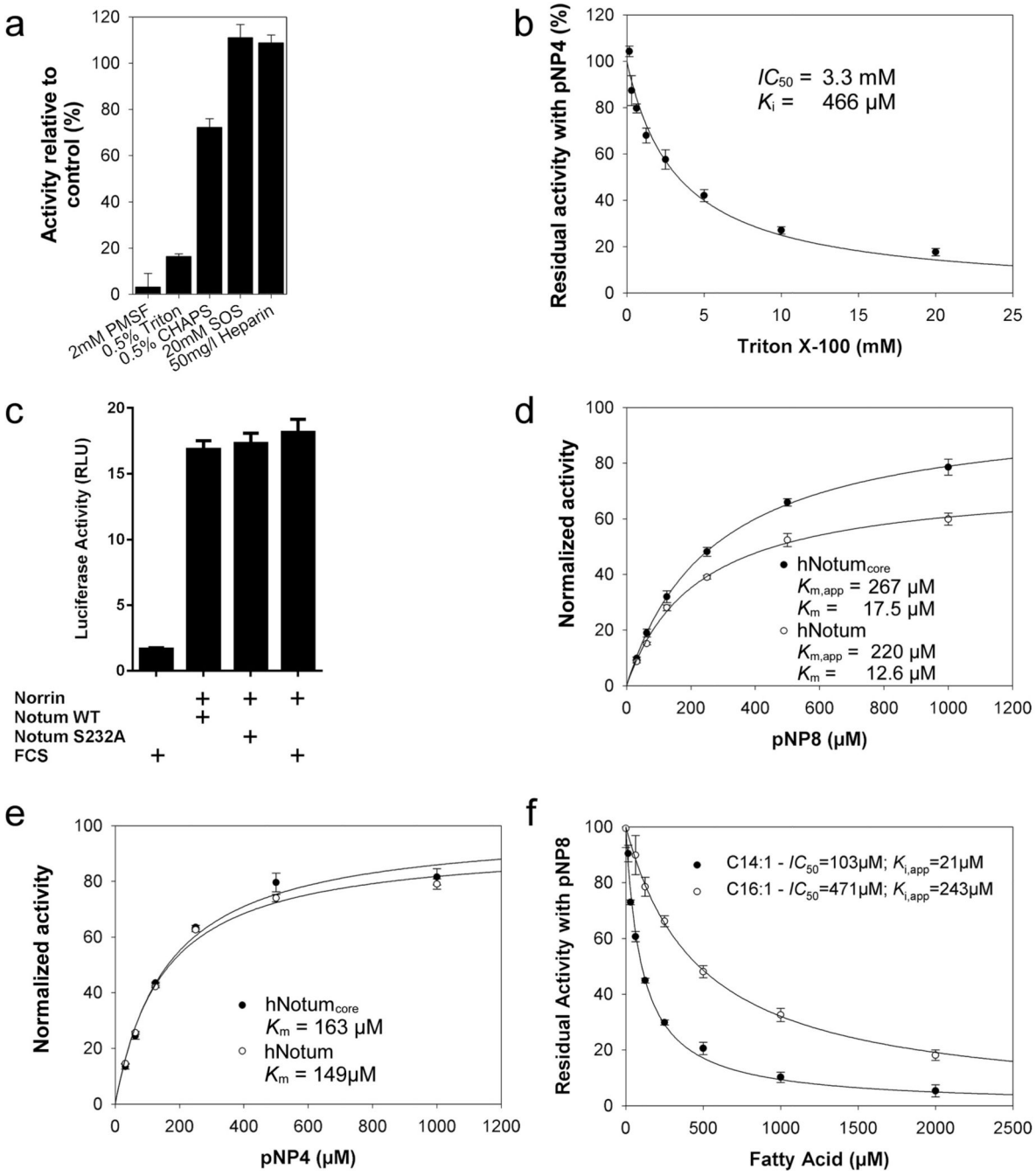

Extended Data Figure 8. Substrates and inhibitors of hNotum

a, Inhibition of hNotum activity on pNP-butyrate (pNP4) by PMSF (30 min preincubation with 2 mM) as well as by Triton X-100 and CHAPS (0.5%). Presence of 20mM sucrose octasulfate (SOS) and 50mg/l Heparin results in a minor increase of esterase activity. Values represent each the activity relative to the mean of four control samples lacking the additives. **b,** Saturable inhibition of hNotum by Triton X-100. Triton X-100 inhibits many esterases due to binding to the acyl binding pocket through its hydrophobic group. **c,** Lack of inhibition of Norrin-mediated β-catenin stabilization by Notum. Recombinant Norrin was

pretreated with hNotum$_{core}$ at a concentration sufficient to suppress Wnt3a-mediated signalling. **d, e,** Saturation kinetics of hNotum's action on pNP-octanoate (pNP8, d) and pNP -butyrate (pNP4, e). The activity was normalized to the A_{max} calculated for hNotum$_{core}$. The activity values for the larger, full length protein were adjusted to compensate for the increased mass. Apparent K_m values in (d) were corrected for the inhibition caused by Triton X-100. **f,** Saturation inhibition kinetics with myristoleic and palmitoleic acid. pNP8 was used at a concentration of 1mM and 250μM, respectively.

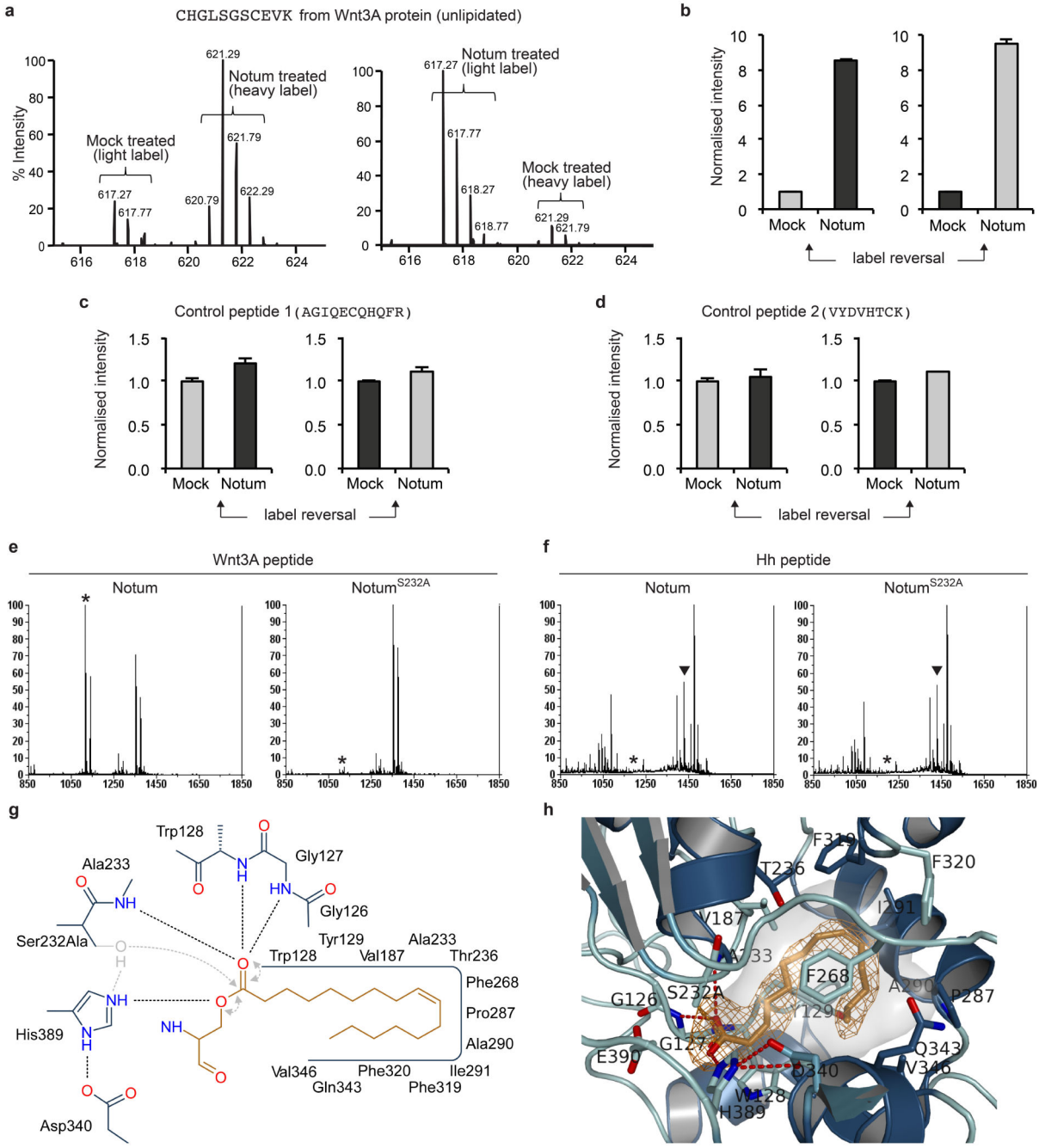

Europe PMC Funders Author Manuscripts

Extended Data Figure 9. Additional mass spectrometric analysis of hNotum's deacylase activity

a, Mass spectra of CHGLSGSCEVK from trypsinised Wnt3A protein mock-treated or treated with $hNotum_{core}$. Left hand graph is the same as that shown in Fig. 5a, while the right hand side shows the results of a separate experiment performed with the labels reversed. **b,** Triplicate LC-MS peak areas with label reversal. Irrespective of the nature of the label (grey indicates light label and black, heavy label), $hNotum_{core}$ triggered an increase in peak area of the delipidated Wnt3A tryptic peptide. **c, d,** Two control Wnt3A cysteine-containing peptides from the same dataset were not affected by $hNotum_{core}$. **e,** Activity of $hNotum_{core}$ and its S232A variant on a synthetic disulphide bonded Wnt3A peptide (CHGLSGSCEVK) palmitoleoylated on the first Serine. Both lipidated and unlipidated peptide could be detected by MALDI-TOF. Incubation with $hNotum_{core}$, but not its S232A variant, caused significant delipidation (peak corresponding to delipidated peptide is marked by asterisk). Quantification of duplicate such experiments is shown in Fig. 5c. **f,** MALDI-TOF analysis shows that neither $hNotum_{core}$ nor its S232A variant delipidated a synthetic Sonic Hedgehog peptide (CGPGRGFGKRR) palmitoylated on its amino terminal Cysteine. Quantification of duplicate such experiments is shown on Fig 5d (peak corresponding to lipidated peptide is marked by black triangle). **g**, 2D active site schematic relating to Fig. 5e. Additional hydrogen bonds and electron pair movements thought to occur during hydrolysis by the wild type are shown in grey. **h,** Close-up view on the myristoleate active site complex of $hNotum_{core}$ (crystal form I). The experimental omit electron density is contoured at 2σ.

Supplementary Material

Refer to Web version on PubMed Central for supplementary material.

Acknowledgements

We thank Kevin Dingwell for supplying purified mWnt3A, Hugo Bellen for anti-Senseless, Cyrille Alexandre for plasmids and advice, Wengang Chai for glycosaminoglycan probes, Tony Holder for suggestions, T. Malinauskas and Carmen Lorenz for advice and technical support, T. Walter for technical support with crystallization, W. Lu and Y. Zhao for help with tissue culture, and the organisers of the Wnt EMBO meeting 2012 where our collaboration began. We thank staff at Diamond Light Source beamlines (i02, i03, i04, i04-1, i24) for assistance with data collection (proposal mx8423). This work was supported by the MRC (U117584268 to JPV; G0900084 to EYJ), the UK Research Council Basic Technology Initiative (Glycoarrays Grant GRS/79268 and EPSRC Translational Grant EP/G037604/1), the Wellcome Trust (Biomedical Resource Grants WT093378MA and WT099197MA) to TF, the European Union (ERC grant WNTEXPORT; 294523 to JPV, a Marie Curie IEF grant to MZ), Cancer Research UK (C375/A10976 to EYJ), and the Japan Society for the Promotion of Science (to SK). THC was funded by a Nuffield Department of Medicine Prize Studentship in conjunction with Clarendon and Somerville College Scholarships. The Wellcome Trust Centre for Human Genetics is supported by Wellcome Trust Centre grant 090532/Z/09/Z.

References

1. Freeman M. Feedback control of intercellular signalling in development. Nature. 2000; 408:313–319. [PubMed: 11099031]
2. Takada R, et al. Monounsaturated fatty acid modification of Wnt protein: its role in Wnt secretion. Dev. Cell. 2006; 11:791–801. [PubMed: 17141155]
3. Janda CY, Waghray D, Levin AM, Thomas C, Garcia KC. Structural basis of Wnt recognition by Frizzled. Science. 2012; 337:59–64. [PubMed: 22653731]
4. Willert K, et al. Wnt proteins are lipid-modified and can act as stem cell growth factors. Nature. 2003; 423:448–452. [PubMed: 12717451]

5. Tang X, et al. Roles of N-glycosylation and lipidation in Wg secretion and signaling. Dev. Biol. 2012; 364:32–41. [PubMed: 22285813]
6. Clevers H, Nusse R. Wnt/& beta-Catenin Signaling and Disease. Cell. 2012; 149:1192–1205. [PubMed: 22682243]
7. Kim SE, et al. Wnt Stabilization of β–Catenin Reveals Principles for Morphogen Receptor-Scaffold Assemblies. Science. 2013; 340:867–870. [PubMed: 23579495]
8. Niehrs C. The complex world of WNT receptor signalling. Nature Rev. Mol. Cell Biol. 2012; 13:767–779. [PubMed: 23151663]
9. Zhang X, et al. Tiki1 is required for head formation via Wnt cleavage-oxidation and inactivation. Cell. 2012; 149:1565–1577. [PubMed: 22726442]
10. Giraldez AJ, Copley RR, Cohen SM. HSPG modification by the secreted enzyme Notum shapes the Wingless morphogen gradient. Dev. Cell. 2002; 2:667–676. [PubMed: 12015973]
11. Gerlitz O, Basler K. Wingful, an extracellular feedback inhibitor of Wingless. Genes & Dev. 2002; 16:1055–1059. [PubMed: 12000788]
12. Filmus J, Capurro M, Rast J. Glypicans. Genome Biol. 2008; 9:224. [PubMed: 18505598]
13. Yan D, Lin X. Shaping morphogen gradients by proteoglycans. Cold Spring Harb Perspect Biol. 2009; 1:a002493. [PubMed: 20066107]
14. Bornemann DJ, Duncan JE, Staatz W, Selleck S, Warrior R. Abrogation of heparan sulfate synthesis in Drosophila disrupts the Wingless, Hedgehog and Decapentaplegic signaling pathways. Development. 2004; 131:1927–1938. [PubMed: 15056609]
15. Kreuger J, Perez L, Giraldez AJ, Cohen SM. Opposing activities of Dally-like glypican at high and low levels of Wingless morphogen activity. Dev. Cell. 2004; 7:503–512. [PubMed: 15469839]
16. Traister A, Shi W, Filmus J. Mammalian Notum induces the release of glypicans and other GPI-anchored proteins from the cell surface. Biochem J. 2008; 410:503–511. [PubMed: 17967162]
17. Häcker U, Nybakken K, Perrimon N. Heparan sulphate proteoglycans: the sweet side of development. Nature Rev Mol. Cell Biology. 2005; 6:530–541.
18. Petersen CP, Reddien PW. Polarized notum activation at wounds inhibits Wnt function to promote planarian head regeneration. Science. 2011; 332:852–855. [PubMed: 21566195]
19. Chang MV, Chang JL, Gangopadhyay A, Shearer A, Cadigan KM. Activation of wingless targets requires bipartite recognition of DNA by TCF. Current Biol. 2008; 18:1877–1881.
20. Flowers GP, Topczewska JM, Topczewski J. A zebrafish Notum homolog specifically blocks the Wnt/β-catenin signaling pathway. Development. 2012; 139:2416–2425. [PubMed: 22669824]
21. Torisu Y, et al. Human homolog of NOTUM, overexpressed in hepatocellular carcinoma, is regulated transcriptionally by beta-catenin/TCF. Cancer Science. 2008; 99:1139–1146. [PubMed: 18429952]
22. Baena-López LA, Nojima H, Vincent J-P. Integration of morphogen signalling within the growth regulatory network. Current Opinion in Cell Biology. 2012; 24:166–172. [PubMed: 22257639]
23. Alberts, Lewis, Johnson, Raff. Molecular Biology of the Cell. 2008
24. Basler K, Struhl G. Compartment boundaries and the control of Drosophila limb pattern by hedgehog protein. Nature. 1994; 368:208–214. [PubMed: 8145818]
25. Alexandre C, Jacinto A, Ingham PW. Transcriptional activation of hedgehog target genes in Drosophila is mediated directly by the cubitus interruptus protein, a member of the GLI family of zinc finger DNA-binding proteins. Genes & Development. 1996; 10:2003–2013. [PubMed: 8769644]
26. Teleman AA, Cohen SM. Dpp gradient formation in the Drosophila wing imaginal disc. Cell. 2000; 103:971–980. [PubMed: 11136981]
27. Whalen DM, Malinauskas T, Gilbert RJC, Siebold C. Structural insights into proteoglycan-shaped Hedgehog signaling. Proc Natl Acad Sci USA. 2013; 110:16420–16425. [PubMed: 24062467]
28. Belenkaya TY, et al. Drosophila Dpp morphogen movement is independent of dynamin-mediated endocytosis but regulated by the glypican members of heparan sulfate proteoglycans. Cell. 2004; 119:231–244. [PubMed: 15479640]
29. Lum L, et al. Identification of Hedgehog pathway components by RNAi in Drosophila cultured cells. Science. 2003; 299:2039–2045. [PubMed: 12663920]

30. Akiyama T, et al. Dally regulates Dpp morphogen gradient formation by stabilizing Dpp on the cell surface. Developmental biology. 2008; 313:408–419. [PubMed: 18054902]
31. You J, Belenkaya T, Lin X. Sulfated is a negative feedback regulator of wingless in Drosophila. Dev. Dynamic. 2011; 240:640–648.
32. Kirkpatrick CA, Dimitroff BD, Rawson JM, Selleck SB. Spatial regulation of Wingless morphogen distribution and signaling by Dally-like protein. Dev. Cell. 2004; 7:513–523. [PubMed: 15469840]
33. Baeg GH, Perrimon N. Functional binding of secreted molecules to heparan sulfate proteoglycans in Drosophila. Current Opinion in Cell Biology. 2000; 12:575–580. [PubMed: 10978892]
34. Nardini M, Dijkstra BW. Alpha/beta hydrolase fold enzymes: the family keeps growing. Current Opinion in Structural Biology. 1999; 9:732–737. [PubMed: 10607665]
35. Krissinel E, Henrick K. Secondary-structure matching (SSM), a new tool for fast protein structure alignment in three dimensions. Acta crystallographica. Section D, Biological crystallography. 2004; 60:2256–2268.
36. Wu D, et al. Crystal structure of human esterase D: a potential genetic marker of retinoblastoma. The FASEB journal. 2009; 23:1441–1446. [PubMed: 19126594]
37. Duncan JA, Gilman AG. A cytoplasmic acyl-protein thioesterase that removes palmitate from G protein alpha subunits and p21(RAS). The Journal of Biol. Chemistry. 1998; 273:15830–15837.
38. Laskowski RA, Watson JD, Thornton JM. ProFunc: a server for predicting protein function from 3D structure. Nucleic Acids Research. 2005; 33:W89–93. [PubMed: 15980588]
39. Orfila C, et al. Expression of mung bean pectin acetyl esterase in potato tubers: effect on acetylation of cell wall polymers and tuber mechanical properties. Planta. 2012; 236:185–196. [PubMed: 22293853]
40. Xu Q, et al. Vascular development in the retina and inner ear: control by Norrin and Frizzled-4, a high-affinity ligand-receptor pair. Cell. 2004; 116:883–895. [PubMed: 15035989]
41. Resh MD. Covalent lipid modifications of proteins. Current Biology. 2013; 23:R431–R435. [PubMed: 23701681]
42. Rios-Esteves J, Resh MD. Stearoyl CoA desaturase is required to produce active, lipid-modified Wnt proteins. Cell Reports. 2013; 4:1072–1081. [PubMed: 24055053]
43. Reichsman F, Smith L, Cumberledge S. Glycosaminoglycans can modulate extracellular localization of the wingless protein and promote signal transduction. The Journal of Cell Biology. 1996; 135:819–827. [PubMed: 8909553]
44. Fuerer C, Habib SJ, Nusse R. A Study on the Interactions Between Heparan Sulfate Proteoglycans and Wnt Proteins. Dev. Dynamics. 2010; 239:184–190.
45. Cruciat C-M, Niehrs C. Secreted and transmembrane wnt inhibitors and activators. Cold Spring Harb Perspect Biol. 2013; 5:a015081. [PubMed: 23085770]
46. de Lau W, Peng WC, Gros P, Clevers H. The R-spondin/Lgr5/Rnf43 module: regulator of Wnt signal strength. Genes & Development. 2014; 28:305–316. [PubMed: 24532711]
47. Zebisch M, et al. Structural and molecular basis of ZNRF3/RNF43 transmembrane ubiquitin ligase inhibition by the Wnt agonist R-spondin. Nature Commun. 2013; 4:2787. [PubMed: 24225776]

Methods references

48. Beckett K, et al. Drosophila S2 Cells Secrete Wingless on Exosome-Like Vesicles but the Wingless Gradient Forms Independently of Exosomes. Traffic. 2012; 14:82–96. [PubMed: 23035643]
49. Vincent J-P, Kolahgar G, Gagliardi M, Piddini E. Steep differences in wingless signaling trigger myc-independent competitive cell interactions. Dev. Cell. 2011; 21:366–374. [PubMed: 21839923]
50. Baena-Lopez LA, Alexandre C, Mitchell A, Pasakarnis L, Vincent JP. Accelerated homologous recombination and subsequent genome modification in Drosophila. Development. 2013; 140:4818–4825. [PubMed: 24154526]
51. Yagi R, Mayer F, Basler K. Refined LexA transactivators and their use in combination with the Drosophila Gal4 system. Proc Natl Acad Sci USA. 2010; 107:16166–16171. [PubMed: 20805468]

52. Alexandre C, Baena-Lopez A, Vincent J-P. Patterning and growth control by membrane-tethered Wingless. Nature. 2014; 505:180–185. [PubMed: 24390349]
53. Marois E, Mahmoud A, Eaton S. The endocytic pathway and formation of the Wingless morphogen gradient. Development. 2006; 133:307–317. [PubMed: 16354714]
54. Doering TL, Englund PT, Hart GW. Detection of glycophospholipid anchors on proteins. Current Protocols in Protein Science. 2001 Chapter 12, Unit 12.15.
55. Fukui S, Feizi T, Galustian C, Lawson AM, Chai W. Oligosaccharide microarrays for high-throughput detection and specificity assignments of carbohydrate-protein interactions. Nature Biotech. 2002; 20:1011–1017.
56. Palma AS, Feizi T, Childs RA, Chai W, Liu Y. The neoglycolipid (NGL)-based oligosaccharide microarray system poised to decipher the meta-glycome. Current Opinion in Chem. Biol. 2014; 18:87–94.
57. Aricescu AR, Lu W, Jones EY. A time- and cost-efficient system for high-level protein production in mammalian cells. Acta crystallographica. Section D, Biological crystallography. 2006; 62:1243–1250.
58. Malinauskas T, Aricescu AR, Lu W, Siebold C, Jones EY. Modular mechanism of Wnt signaling inhibition by Wnt inhibitory factor 1. Nature structural & molecular biology. 2011; 18:886–893.
59. Gagliardi M, Hernandez A, McGough IJ, Vincent J-P. Inhibitors of endocytosis prevent Wnt/Wingless signalling by reducing the level of basal β -Catenin/Armadillo. J Cell Sci. 2014; 127:4918–4926. [PubMed: 25236598]
60. Xu H, et al. Tbx1 has a dual role in the morphogenesis of the cardiac outflow tract. Development. 2004; 131:3217–3227. [PubMed: 15175244]
61. Blitzer JT, Nusse R. A critical role for endocytosis in Wnt signaling. BMC Cell Biol. 2006; 7:28. [PubMed: 16824228]

Extended data reference

62. Glise B, et al. Shifted, the Drosophila ortholog of Wnt inhibitory factor-1, controls the distribution and movement of Hedgehog. Dev. Cell. 2005; 8:255–266. [PubMed: 15691766]

Europe PMC Funders Author Manuscripts

Europe PMC Funders Author Manuscripts

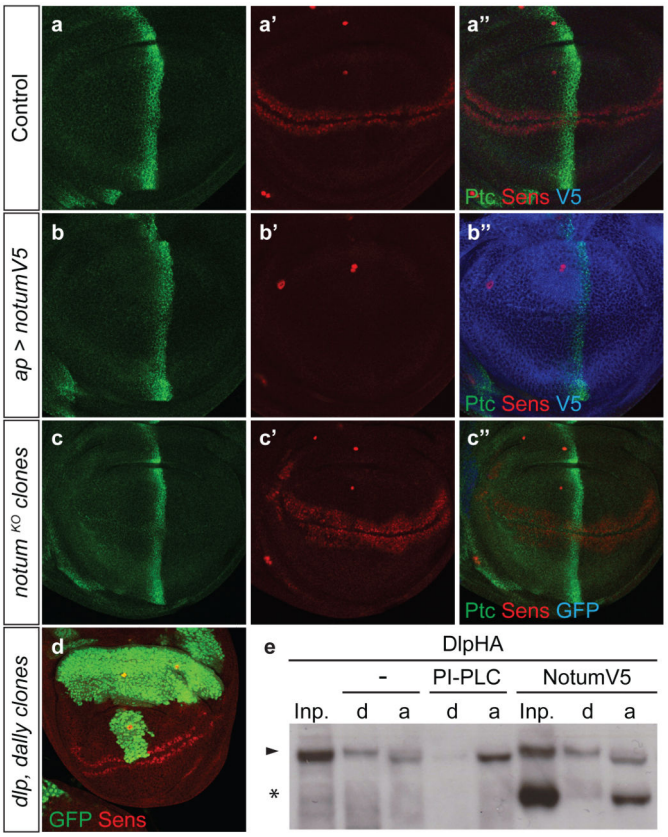

Figure 1. Notum specifically inhibits Wnt signalling

a-c, Overexpression of V5-tagged dNotum with the *apterous-gal4* driver, which is expressed in the dorsal compartment prevents expression of Senseless (Sens) but not that of Patched (Ptc) (b). Loss of *notum* activity, achieved by generating large patches of *notum*^{KO} tissue (See Methods), marked by the loss of GFP, leads to broadening of Senseless expression but does not affect Patched expression. As in all subsequent confocal images, 3rd instar wing imaginal discs are shown with posterior to the right and dorsal up. **d**, Senseless is expressed seemingly normally in large patches of *dlp dally* mutant cells (GFP negative) **e**, Western blot (co-stained with anti-V5 and anti-HA) of phase separated extracts of S2 cells transfected with a plasmid expressing haemagglutinin (HA)-tagged Dlp. In control extracts, Dlp (arrowhead) is found equally in the detergent (d) and aqueous (a) phases. Coexpression of dNotum-V5 (asterisk) had no impact while treatment with PIPLC shifted Dlp to the aqueous phase.

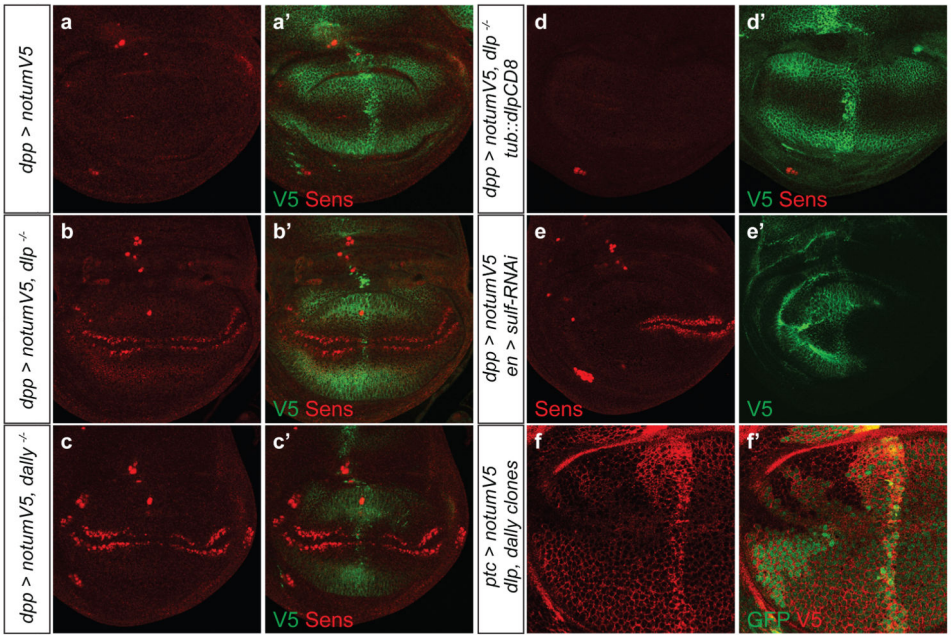

Figure 2. Notum requires the GAGs of glypicans to inhibit Wingless signalling

a-c, Ectopically expressed dNotum-V5 does not suppress Senseless expression in the absence of *dlp* (b) or *dally* (c). Although dNotum is only expressed in a vertical band along the A-P boundary, it spreads along the whole A-P axis. **d,** Ectopic dNotum represses Senseless expression in *dlp* mutants that express Dlp-CD8 (*tubulin* promoter). **e**, Expression of an RNAi transgene against *sulfateless* in the posterior compartment prevents dNotum-V5 (expressed from *dpp-lexA lex-op-notum-V5)* from being retained at the cell surface and from suppressing Senseless expression. Wingless signalling is still suppressed in the anterior compartment. **f,** Accumulation of dNotum-V5 is reduced at the surface of *dlp dally* double mutant tissue (GFP-negative).

Europe PMC Funders Author Manuscripts

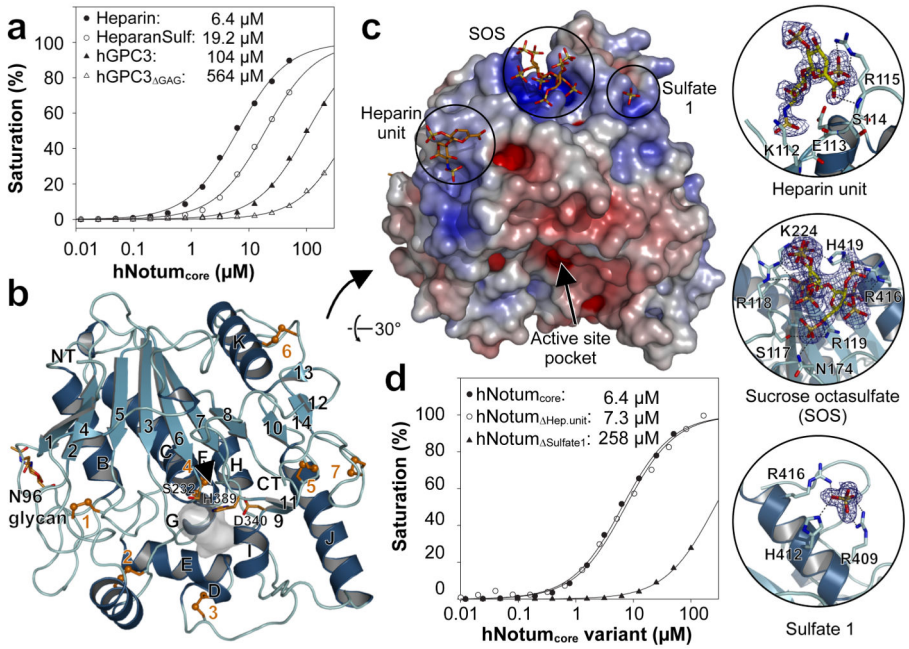

Figure 3. hNotum structure and GAG binding

a, Binding of $hNotum_{core}$ to immobilized heparin, heparan sulfate (HeparanSulf), hGPC3 or $hGPC3_{\Delta GAG}$, assayed by SPR. **b,** Structure of hNotum. β-strands are numbered and α-helices are labelled alphabetically from N to C terminus. Disulfides are shown in orange, catalytic triad residues as sticks and the active site pocket shaded grey. N96 is glycosylated (also in dNotum). **c,** Heparin-mimicking ligands from three different structures are plotted onto a surface representation coloured by electrostatic potential from red ($-8k_bT/e_c$) to blue ($-8k_bT/e_c$). Close-up views of binding sites are shown on the right with experimental omit electron density contoured at 2.0σ. **d,** SPR assay measuring $hNotum_{core}$ variant binding to immobilized heparin. Mutation of the heparin disaccharide binding site (R115S; $hNotum_{\Delta Hep.unit}$) had little effect while mutations in the sulfate binding site 1 (R409Q H412N R416Q; $hNotum_{\Delta Sulfate1}$) strongly reduced binding. For SPR (a, d), each data point is the mean result of two replicates.

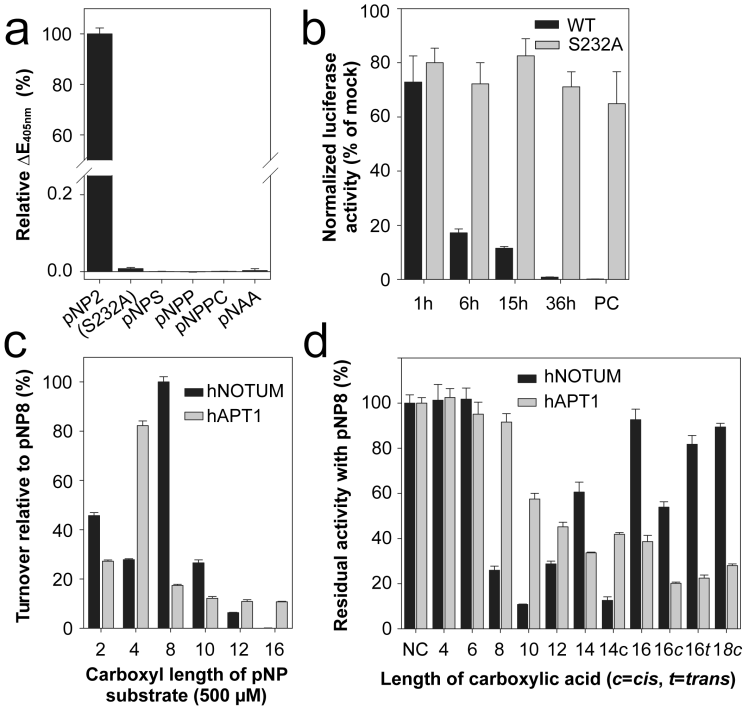

Figure 4. Enzymatic activity of hNotum

a, Activity of $hNotum_{core}$ and its S232A variant on p-nitrophenyl (pNP) acetate (pNP2) and activity of $hNotum_{core}$ on other chromogenic substrates. pNPS = pNP-sulfate (sulfatase substrate); pNPP=pNP-phosphate (phosphatase substrate); pNPPC=pNP-phosphorylcholine (phospholipase C substrate); pNAA=*p*-Nitroacetanilide (amidase/protease substrate). **b,** mWnt3A inactivation by hNotum. After the indicated time, $hNotum_{core}$ or its S232A variant was removed with cobalt affinity beads and residual Wnt3A activity measured with TOPFlash. PC = no hNotum removal. Results are normalised to those from identically treated mock samples. **c,** Activity of hNotum and hAPT1 on chromogenic *p*-nitrophenyl ester substrates of different lengths. **d,** Inhibition of hNotum by various carboxylic acids. pNP8 was used as substrate at a concentration of 1 mM as were the carboxylic acids. c, t: *cis* or *trans* C9-C10 double bond. All graphs show the mean +/− s.d. (n=4).

Europe PMC Funders Author Manuscripts

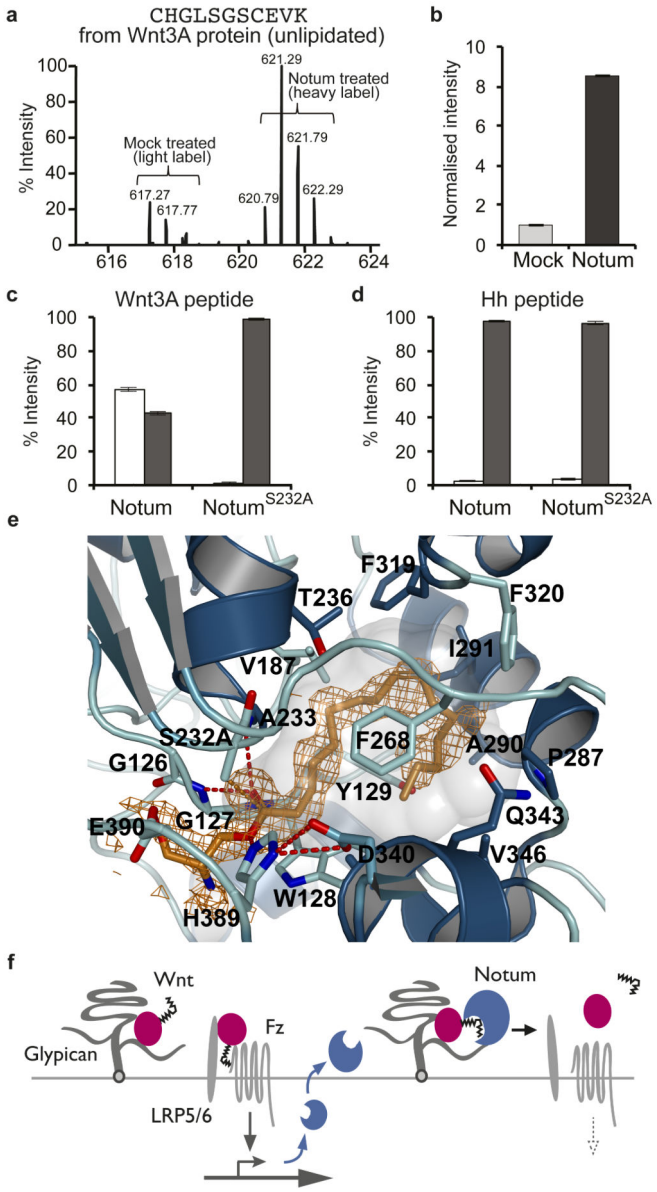

Figure 5. Wnt-deacylation by Notum

a, LC-MS analysis of mWnt3A protein treated with $hNotum_{core}$ or a mock solution. By comparison to mock treatment (light label), addition of hNotum (heavy label) caused a significant increase in the signal intensity of unlipidated CHGLSGSCEVK **b,** LC-MS peak areas from panel a.; shown as mean +/− s.e.m. (n=3) **c, d,** Quantification from MALDI analysis of synthetic lipid-bearing peptides treated with $hNotum_{core}$ or its S232A variant; shown as mean +/− s.e.m. (n=3). Palmitoleoylated hWnt3A peptide, but not palmitoylated hSonic Hedgehog peptide, was specifically deacylated by the wild type enzyme. **e,** Close-up view on the seryl-palmitoleate active site complex of hNotum. The experimental omit electron density is contoured at 2σ. **f,** Feedback control by Notum. Notum deacylates Wnt in a Glypican-assisted fashion.